

Synthesis of alnustone-like diarylpentanoids via a 4 + 1 strategy and assessment of their potential anticancer activity

Neslihan ÇELEBİOĞLU¹ , Özlem ÖZDEMİR TOZLU² , Hasan TÜRKEZ³ , Hasan SEÇEN^{1,*} 

¹Department of Chemistry, Faculty of Sciences, Atatürk University, Erzurum, Türkiye

²Department of Molecular Biology and Genetics, Erzurum Technical University, Erzurum, Türkiye

³Department of Medical Biology, Faculty of Medicine, Atatürk University, Erzurum, Türkiye

Received: 01.06.2023

Accepted/Published Online: 11.10.2023

Final Version: 31.10.2023

Abstract: Twelve compounds with a 1,5-diaryl-1-penten-3-one structure were synthesized and their cytotoxic activities were evaluated. The 1,5-diaryl-1-penten-3-one compounds were obtained via in situ enaminations of 4-phenyl-2-butanone and 4-(4-hydroxyphenyl)-2-butanone in the presence of pyrrolidine-AcOH, followed by condensation with six different benzaldehydes. The synthesized compounds were tested for their cytotoxic activity against human glioblastoma (U87-MG), breast (MCF-7), and prostate (PC-3) cancer cell lines. Some of the novel compounds exhibited remarkable cytotoxic action, especially against MCF-7 cancer cells.

Keywords: 1,5-Diarylpentanoid, cytotoxic activity, breast cancer, prostate cancer, glioblastoma, anticancer effect

1. Introduction

Diarylheptanoids, a special group of natural products, are ArC₇Ar structured compounds bearing aryl groups at positions C-1 and C-7. These compounds contain C=C, C=O, and OH groups in the heptane chain [1,2]. Natural diarylheptanoids have a great variety of biological and pharmaceutical properties and are therefore recognized as promising therapeutic agents [3,4]. Curcumin (**1**), found in the rhizomes of *Curcuma longa* at a ratio of 3%–5%, is the most widely known natural diarylheptanoid and is the main component of turmeric, a dietary ingredient (Figure 1). Numerous studies have been performed on the biological effects of curcumin (**1**), which include antiinflammatory, immunomodulatory, antibacterial, antiischemic, anticarcinogenic, hepatoprotective, nephroprotective, hypoglycemic, and antirheumatic properties [5].

Diarylpentanoids ArC₅Ar are two carbonless analogs of diarylheptanoids. Most of these compounds, which have been discovered in recent years, constitute a small group of natural products. To date, nearly 30 diarylpentanoid compounds with different structures have been isolated from nature, their structures have been elucidated, and the biological activities of some of them have been investigated. The isolation and biological activities of 20 diarylpentanoid compounds were described for the first time in a review article by our group in 2017 [6]. Natural diarylpentanoids have been shown to have a wide range of biological effects including anticancer, antiviral, antioxidant, cytotoxic, anti-HIV, nematocidal, antiviral, immunomodulatory, antifeedant, and NO inhibitory effects [6].

Since 1962, when the first natural diarylpentanoid was isolated from nature, they have attracted intense interest as mono-carbonyl analogs of curcumin. In this regard, more than 600 synthetic diarylpentanoid derivatives have been synthesized, and these chemicals have undergone extensive bioactivity studies, with a focus on their anticancer activity. Numerous studies have reported that diarylpentanoid derivatives exhibit a wide range of biological activities including antiviral, antimalarial, and chemopreventive and antitumoral properties [7–11]. The available data support the theory that diarylpentanoid derivatives affect a wide range of biochemical and molecular cascades. In a review article, Moreira et al. [12] examined the structure–activity relationships of synthetic diarylpentanoids in terms of antitumor activity against multiplexed cancer types including glioblastoma (GBM), prostate, and breast cancers. The meta-hydroxyl and adjacent dimethoxyl groups containing diarylpentanoids were found to be cytotoxic and were considered as novel sources of novel anticancer agents [13]. The vast majority of the synthetically prepared diarylpentanoids whose activities have been investigated are 1,4-pentadiene-3-one structured curcumin-like compounds (Figure 1) [12].

Alnustone (**2**), a natural diarylheptanoid, has attracted interest due to its wide range of biological properties, such as its antiinflammatory, antiemetic, antihepatotoxic, and anticancer properties (Figure 1) [14].

* Correspondence: hsecen@atauni.edu.tr

In a previous study, it was shown that alnustone-like compounds exhibit stronger antitumor activity than tamoxifen and paclitaxel, which were used as reference drug compounds against the MCF-7 cell line [15].

Artamenone, 1,5-bis-(4-hydroxyphenyl)-2-penten-3-one, a natural diarylheptanoid [16,17], is similar to alnustone (2) due to its $\text{ArCH}_2\text{CH}_2\text{C}(\text{O})\text{CH}=\text{CHAr}$ pharmacophore group.

Brain tumor incidence has increased over the past few decades [18]. An estimated 308,102 people received a primary brain or spinal cord tumor diagnosis globally in 2020 [19]. The microglial cell subtype known as astrocytes is the source of the solid tumor known as GBM, which develops in the brain or spinal cord [20]. The capacity of GBM to invade healthy tissues due to the maintenance of continuous angiogenesis makes it the most aggressive type of brain tumor. With a global incidence of fewer than 10 per 100,000 people, GBM is also the most common primary brain tumor, accounting for about 15% of all primary brain tumors in adults [21–23]. GBM also has poor prognosis and a higher fatality rate than other types of brain tumors [24].

In 2020, breast cancer was considered the most frequently diagnosed cancer worldwide. Since 2.3 million new cases of breast cancer (11.7% of the total) were estimated globally in that year, the incidence of breast cancer has overtaken that of lung cancer. Additionally, it contributed to 685,000 deaths from cancer in 2020 and was the sixth highest cause of cancer mortality globally [25,26]. The prevalence of this malignancy has dramatically grown in recent decades, particularly in some areas such as Europe. The determination of risk factors and primary prevention measures to reduce exposure are crucial components of controlling this trend, since the incidence of breast cancer is anticipated to continue rising in the future [27]. Similarly, as one of the most prevalent cancers in men, prostate cancer affects about one in six men, making it a serious public health concern. According to the World Health Organization (WHO), with 1,414,259 new cases worldwide, prostate cancer was the second most common illness and the fifth largest cause of cancer-related deaths among men [28].

In the literature, intensive studies have been carried out on the synthesis and bioactivities of curcumin-like diarylpentanoids. However, there are no such studies on alnustone-type diarylpentanoids. In this study, we present a methodology for the synthesis of alnustone-type diarylpentanoids containing $\text{ArCH}_2\text{CH}_2\text{C}(\text{O})\text{CH}=\text{CHAr}$ pharmacophore groups in addition to assessing their cytotoxic activity against the U87-MG, MCF-7, and PC-3 cancer cell lines (Figure 2).

2. Results and discussion

Retrosynthetic analysis carried out to synthesize the 1,5-diaryl-1-penten-3-one structures **5a–5l** showed that these compounds can be obtained by combining 4-aryl-2-butanones (4 C) with aryl aldehydes (1 C) by condensation under suitable conditions ($4 + 1 = 5$) (Figure 3).

As shown in Figure 3, the target compounds can be obtained by the condensation of benzaldehydes with 4-aryl-2-butanones. However, this condensation process cannot be carried out by classical Claisen–Schmidt condensation because self-condensation and the Cannizzaro reaction can occur under strong basic conditions. In our previous studies [15,29–31], alnustone itself and alnustone-type diarylheptanoids were successfully synthesized by the condensation of 4-aryl-2-butanones and cinnamaldehydes in the presence of AcOH and pyrrolidine (via in situ enamination). In light of this, similar reaction conditions were applied for the synthesis of 1,5-diaryl-1-penten-3-ones **5a–5l**. For this purpose, AcOH and pyrrolidine were added to 4-phenylbutan-2-one (**6**) and 4-(4-hydroxyphenyl)butan-2-one (**7**) in dry diethyl ether

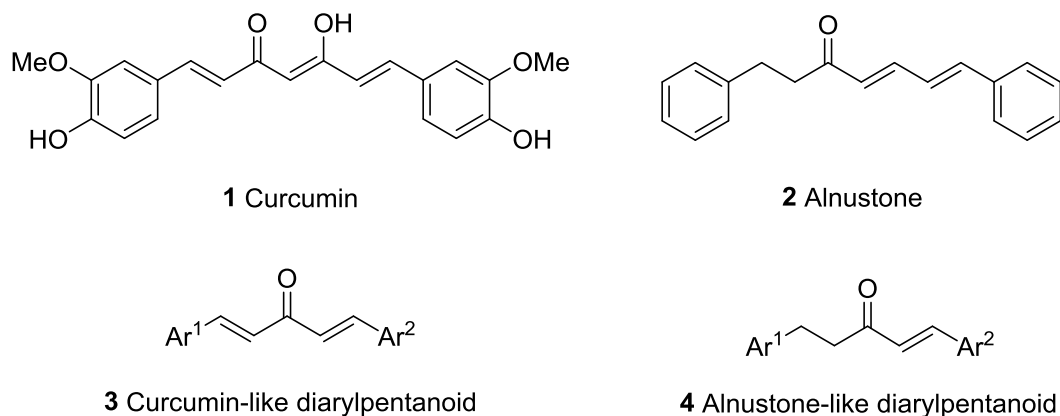


Figure 1. Curcumin (1), alnustone (2), and related diarylpentanoids (3, 4).

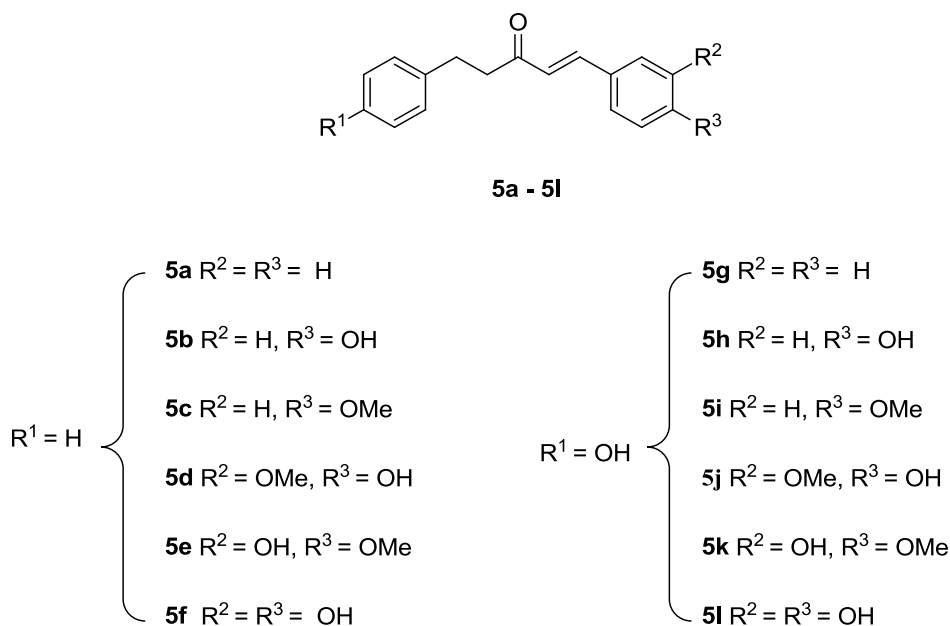


Figure 2. The synthesized alnustone-like diarylpentanoids (5a–5l).

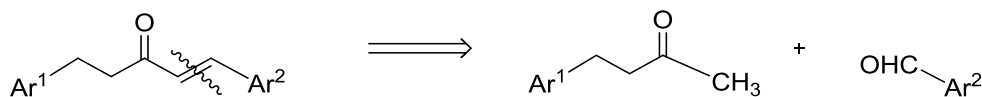


Figure 3. Retrosynthetic analysis of 1,5-diaryl-pent-1-en-3-ones 5a–5l.

(Et₂O) or tetrahydrofuran (THF) at 0 °C and stirred for 30 min. Benzaldehydes were then added and stirred for 48–60 h. Thus, 12 target molecules (5a–5l) in the structure of the 1,5-diaryl-1-penten-3-ones were obtained in yields ranging from 25% to 53% (Figure 4).

The structures of the synthesized compounds (5a–5l) were elucidated based on hydrogen-1 NMR (¹H NMR), carbon-13 NMR (¹³C NMR), high-resolution mass spectrometry (HRMS), and microanalysis. In the ¹H NMR spectra of the synthesized compounds, all of the H-C(1) and H-C(2) hydrogens resonated as an AX system. The H-C(1) and H-C(2) hydrogens were a conjugated α,β-unsaturated alkene system. Therefore, while the H-C(1) hydrogens representing the A part of the AX system resonated at δ = 7.58–7.46 ppm (downfield) as a doublet, the H-C(2) hydrogens representing the X system resonated between δ = 6.74 and 6.56 ppm (upfield) as a doublet. The *J*_{1,2} values ranged between 15.5 and 16.4 Hz, indicating that the alkene structures in all of the compounds were formed as the *E* configuration (trans), as generally expected. The H₂C(4) and H₂C(5) hydrogens arose as an A₂B₂ system in the aliphatic region between δ = 3.02 and 2.90 ppm. While the phenyl rings resonated as multiplets in the aromatic region, 4-substituted phenyls resonated as an AA'XX' system and the 3,4-disubstituted phenyls arose as ABX systems in the aromatic region.

As with the ¹H NMR spectra, the ¹³C NMR spectra of the 1,5-diaryl-1-penten-3-one compounds were in complete agreement with the structure. Namely, the C-3 ketone carbons resonated at δ = 201.7–199.6 ppm, C(1) carbons resonated at δ = 144.5–141.9 ppm, C(2) carbons resonated at δ = 126.4–122.4 ppm, C(5) carbons resonated at δ = 30.6–29.4 ppm, and C(4) carbons resonated at δ = 42.9–41.9 ppm. The carbons belonging to the Ar¹ and Ar² ring systems also resonated in the olefinic/aromatic region in accordance with their structures.

GBM (U87-MG), breast cancer (MCF-7), prostate carcinoma (PC-3), and lung epithelium (HPAEPiC) cell lines were used to assess the cytotoxic action potential of compounds 5a–5l. The cells were grown in a single layer in flasks in appro-

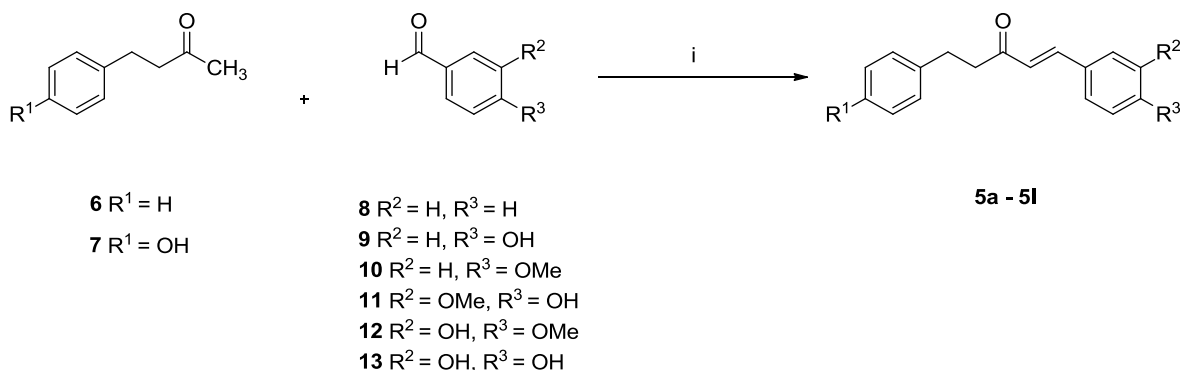


Figure 4. Syntheses of compounds **5a–5l**: i) pyrrolidine, AcOH, dry Et₂O or dry THF, 0 °C, N₂ atm, 30 min; and then rt, 48–60 h, ~25%–53%.

appropriate medium containing 10% fetal bovine serum (FBS), 1% penicillin/streptomycin, and 1% L-glutamine at 37 °C and 5% CO₂ to maintain the pH balance. Cells that had reached 70%–80% confluence were used in the experiments.

The 3-(4,5-dimethylthiazol-2-yl)-2,5-diphenyltetrazolium bromide (MTT) method is a widely used colorimetric method for the quantitative determination of cell viability. It is based on the reduction of the tetrazolium ring of the yellow dye MTT by living cells. As a result of the reduction, the tetrazolium ring breaks down to form a dark blue-violet formazan compound. Cell viability is then determined spectrophotometrically. The viability of untreated cells is assumed to be 100% and the viability of treated cells is determined as a percentage (%) according to those cells.

To each 96-well plate, 2 × 10⁴ cells were seeded and treated with 6 different concentrations (3.125, 6.25, 12.5, 25, 50, and 100 mg/L) of the 12 tested compounds, and then the plates were incubated in a CO₂ oven at 37 °C for 48 h. At the end of the incubation, 10 µL of the MTT mixture was added to each well using a pipette, which was then gently mixed for 1 min on a circular mixer. The cells were incubated in a CO₂ oven at 37 °C for 3–4 h. The formazan that formed as a result of the incubation was seen as dark crystals at the bottoms of the wells. The culture medium was carefully aspirated from each well without dispersing the cell layer, and then 100 µL of dimethyl sulfoxide (DMSO) was added to each well and gently stirred on an orbital stirrer to dissolve the formazan crystals. Each sample was read at a wavelength of 570 nm in a spectrophotometer and absorbance values were obtained. A wavelength of 630 nm was used as the reference wavelength.

Percent viability and cytotoxicity values for each dose administered were calculated according to the following formulas:

$$\% \text{ Viability} = (\text{absorbance of the sample} / \text{absorbance of the control}) \times 100$$

$$\% \text{ Cytotoxicity} = [1 - (\text{absorbance of the sample} / \text{absorbance of the control})] \times 100$$

The IC₅₀ dose, as the concentration of inhibitor that caused a 50% decrease in cell viability, was calculated using Excel regression analysis.

The cytotoxic activities of diarylpentanoids **5a–5l** against human GBM (U87-MG), breast cancer (MCF-7), prostate cancer (PC-3), and healthy HPAEpiC cells are presented in Table 1.

Compounds **5a**, **5b**, **5d**, **5e**, **5g**, **5h**, and **5i** exerted cytotoxic activity below 30 µM. The IC₅₀ values against three different cancer cells indicated that these molecules can be considered as broad-spectrum anticancer agents. Of the 12 compounds examined, 7 compounds (**5a**, **5b**, **5d**, **5e**, **5g**, **5h**, and **5i**) showed cytotoxicity against MCF-7 cells and 3 compounds (**5b**, **5d**, and **5i**) showed cytotoxicity against PC-3 cells below an IC₅₀ of < 30 µM. Compared to the doxorubicin (DOX) used as a reference, all of the compounds were less active against the GBM U87-MG cell line compared to the others. However, three of the compounds were more active than DOX against the MCF-7 cell line.

Cell morphological characteristics were examined via the fluorescent Hoechst 33258 staining approach. The analysis revealed that there were some alterations in the fluorescent staining characteristics of the treated cells with novel diarylpentanoids **5a–5l**. Hoechst 33258 staining revealed considerable morphological alterations in the nuclear chromatin. The nuclei in the untreated group were stained a less brilliant blue and the color was uniform. After 48 h of treatment at the IC₅₀ concentrations of compounds **5a** and **5i**, the blue emission light in the apoptotic cells was considerably brighter than in the control cells. Many compound-treated cells also had condensed chromatin, and some had the shape of apoptotic bodies, which is one of the basic features of apoptotic cells (Figures 5 and 6). In line with these findings, it was previously reported that the diarylpentanoid BP-M345 exerted potential as an anticancer drug, showing its antiproliferative activity by preventing mitosis through microtubule disruption and inducing cancer cell death [32]. Likewise, diarylpentanoid

Table 1. The IC₅₀ values (in µM) of diarylpentanoids **5a–5l** against human cancer cells and healthy cells for 48 h.

| Compound | U87-MG | MCF-7 | PC-3 | HPAEpiC |
|-----------------|--------|--------|--------|---------|
| DOX control (+) | 8.95 | 14.72 | 6.76 | 64.43 |
| 5a | 107.49 | 11.38 | 50.15 | 84.77 |
| 5b | 70.87 | 9.55 | 22.04 | 5.51 |
| 5c | 213.37 | 50.21 | 438.75 | 92.26 |
| 5d | 31.92 | 27.81 | 20.86 | 14.42 |
| 5e | 133.37 | 21.82 | 95.82 | 26.35 |
| 5f | 33.40 | 544.39 | 97.50 | 43.12 |
| 5g | 127.74 | 16.17 | 290.88 | 21.13 |
| 5h | 357.92 | 26.72 | 436.68 | 51.40 |
| 5i | 233.33 | 5.92 | 9.74 | 14.91 |
| 5j | 75.73 | 35.00 | 32.22 | 93.43 |
| 5k | 52.56 | 202.72 | 45.12 | 69.33 |
| 5l | 286.63 | 317.02 | 184.70 | 395.99 |

derivatives have led to intrinsic apoptosis in cancer cells by upregulating proapoptotic proteins such as Bad and Bax and downregulating prosurvival proteins such as Bcl-2 and Bcl-xL [33]. Their possible molecular targets were associated with the mitogen-activated protein kinase/extracellular signal-regulated kinase (MAPK/ERK), signal transducers and activators of transcription (STAT), and nuclear factor kappa-light-chain-enhancer of activated B cells (NF-κB) signaling pathways that are involved in cancer development and progression [34].

Selectivity, which is the most relevant parameter in determining in vitro anticancer potential, was used to determine the efficacy of the compounds [35,36]. The selectivity index (SI) for each compound was expressed as $SI = IC_{50}$ for normal cells (HPAEpiC)/ IC_{50} for the cancer cell lines (U87-MG, PC-3, and MCF-7) (Table 2).

The HPAEpiC cell line was used as a noncancerous cell line for evaluating the cytotoxicity of the newly synthesized compounds, since epithelial tissues are widespread throughout the body and these cells turnover rapidly and mutations naturally accumulate throughout life. Moreover, epithelial tissue is also considered as the most common site for the development of cancers. In terms of the SI, three of the compounds had good selectivity against the MCF-7 cell line (**5a**: 7.45, **5j**: 2.67, and **5i**: 2.52; reference DOX: 4.38). It is especially noteworthy that compound **5a** had a better SI value against MCF-7 cells than the reference DOX. For PC-3 cells, two compounds (**5j**: 2.90 and **5l**: 2.14) showed high selectivity.

3. Conclusion

In this study, 12 diarylpentanoids in the structures of 1,5-diaryl-1-penten-3-one were realized by condensation of two 4-aryl-2-butanones and six benzaldehydes. The obtained compounds were tested against the U87-MG, MCF-7, and PC-3 cancer cell lines. The synthesized compounds showed broad-spectrum antitumor activity, especially against the MCF-7 cell line. Moreover, compound **5a** showed a better SI value against MCF-7 cells than reference drug DOX. Alnustone and 1,5-diphenyl-1-penten-3-one both contain nonsubstituted phenyl rings and they are structurally very similar to each other. This similarity indicates that the 1,5-diphenyl-1-penten-3-one structure is a very potent pharmacophore group. Collectively, these findings suggest that the alnustone-like diarylpentanoids might be considered as novel sources of effective broad-spectrum anticancer agents and deserve further research.

4. Experimental

All of the reactions were carried out under a nitrogen atmosphere and monitored by thin-layer chromatography (TLC) and NMR spectroscopy. The ¹H NMR and ¹³C NMR spectra were recorded with 400 (100) MHz Bruker (Bruker Corp., Billerica, MA, USA) and Varian (Varian Medical Systems, Palo Alto, CA, USA) instruments. Exchangeable hydrogens or carbons were marked with the same letters. Elemental analyses were recorded using a LECO CHNS-932 elemental analyzer (LECO Corporation, St. Joseph, MI, USA) and HRMS spectra were recorded using an Agilent 6530 LC-MS QTOF (Agilent Technologies, Santa Clara, CA, USA). Melting points were measured using a Gallenkamp melting point device.

Table 2. SI values of diarylpentanoids **5a–5l** against several human cancer cell lines.

| Compound | U87-MG cells | MCF-7 cells | PC-3 cells |
|-----------------|--------------|-------------|------------|
| DOX control (+) | 7.20 | 4.38 | 9.53 |
| 5a | 0.79 | 7.45 | 1.69 |
| 5b | 0.08 | 0.58 | 0.25 |
| 5c | 0.42 | 1.84 | 0.21 |
| 5d | 0.45 | 0.52 | 0.69 |
| 5e | 0.20 | 1.21 | 0.28 |
| 5f | 1.29 | 0.08 | 0.44 |
| 5g | 0.17 | 1.31 | 0.07 |
| 5h | 0.14 | 1.92 | 0.12 |
| 5i | 0.06 | 2.52 | 1.53 |
| 5j | 1.23 | 2.67 | 2.90 |
| 5k | 1.32 | 0.34 | 1.54 |
| 5l | 1.38 | 1.25 | 2.14 |

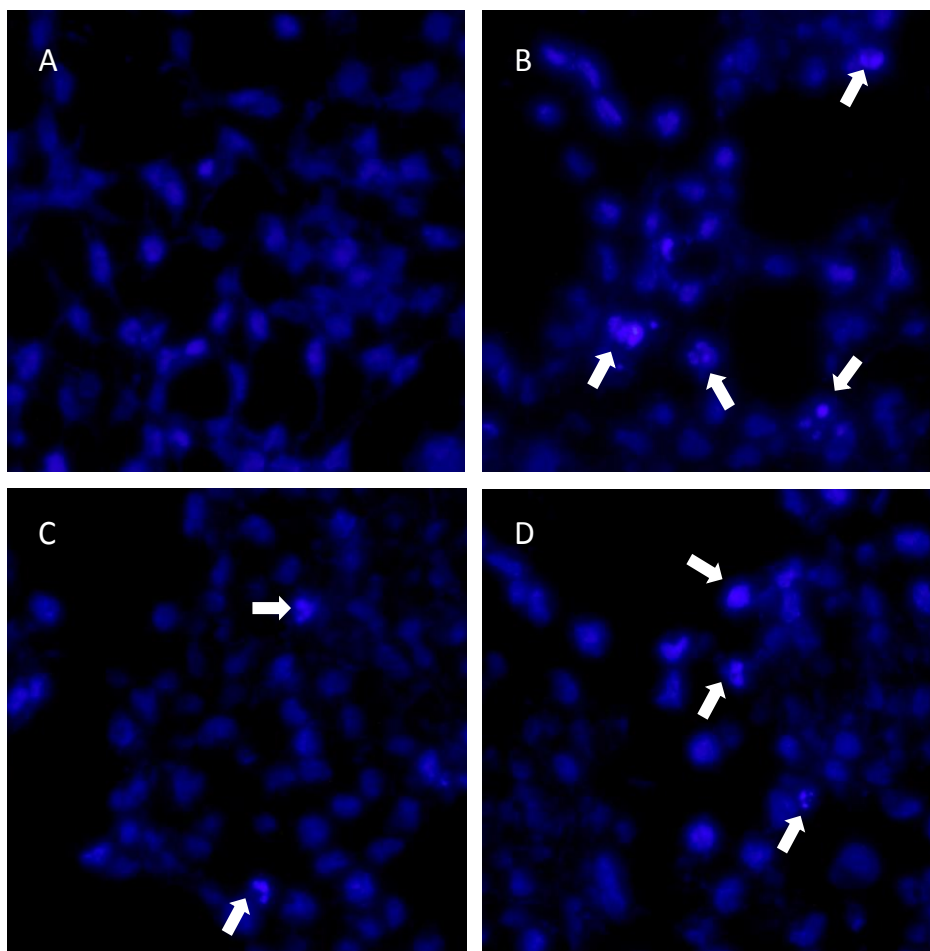


Figure 5. Fluorescent staining of the nuclei in MCF-7 cells by Hoechst 33258. The cells were treated with an IC_{50} concentration of **5a** or **5i** for 48 h. (A) Untreated cells, (B) H_2O_2 -treated cells, (C) **5a**-treated cells, and (D) **5i**-treated cells. Arrows indicate apoptotic cells with fragmented nuclei. Magnification: 400 \times .

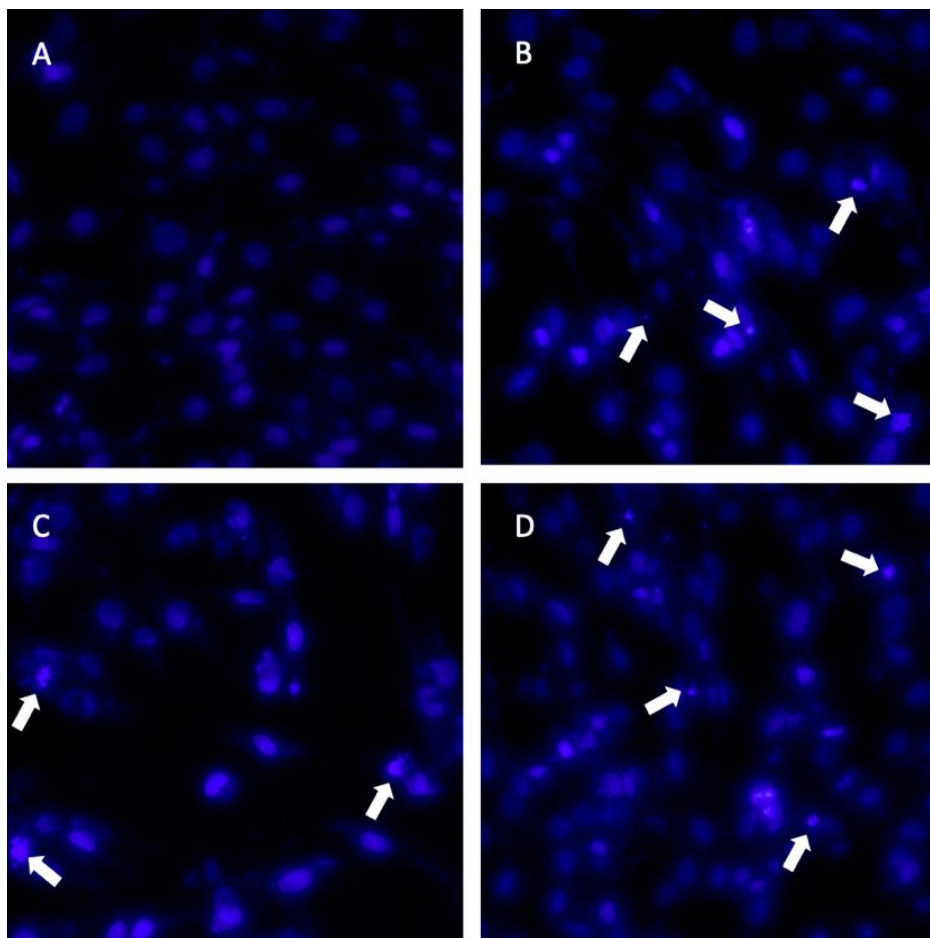


Figure 6. Fluorescent staining of the nuclei in U87-MG cells by Hoechst 33258. The cells were treated with an IC_{50} concentration of **5a** or **5i** for 48 h. (A) Untreated cells, (B) H_2O_2 -treated cells, (C) **5a**-treated cells, and (D) **5i**-treated cells. Arrows indicate apoptotic cells with fragmented nuclei. Magnification: 400 \times .

4.1. General synthetic procedures for the 1,5-diaryl-1-penten-3-ones ((*E*)-1,5-diphenylpent-1-en-3-one (**5a**))

4-Phenylbutan-2-one (**6**) (2.04 g, 13.74 mmol) was dissolved in 5 mL of dry Et_2O at 0 °C under a nitrogen atmosphere. A solution of pyrrolidine (1.07 g, 1.25 mL, 15.11 mmol) and AcOH (0.90 g, 0.86 mL, 15.11 mmol) in 5 mL of dry Et_2O was added dropwise to the reaction medium under the same reaction conditions for 10 min. After stirring for 30 min, the temperature was reduced to 0 °C and a solution of benzaldehyde (**8**) (1.45 g, 13.74 mmol) in 5 mL of Et_2O was added dropwise over 30 min. The reaction mixture was stirred at room temperature for 48 h by monitoring with TLC. To the reaction medium, 10 mL of 1 M HCl solution was added. The crude product was extracted with 2 \times 50 mL of Et_2O and the organic phases were combined. The organic phases were washed with 2 \times 30 mL of H_2O , dried over Na_2SO_4 , and the solvent was evaporated. The crude product was purified by column chromatography on a silica gel column using 6:94 EtOAc-hexane and then crystallized with EtOAc-hexane to give (*E*)-1,5-diphenylpent-1-en-3-one (**5a**) (1.81 g, 56%). R_f (AcOEt/hexanes 1:9): 0.6. White solid. Mp 56–57 °C. 1H NMR (400 MHz, $CDCl_3$): d 7.55 (d, 1H, H-1, $J_{1,2} = 16.2$ Hz), 7.55–7.52 (m, 2H, H-2'/6'), 7.41–7.39 (m, 3H, H-3'/4'/5'), 7.33–7.22 (m, 5H, H-2''/3''/4''/5''/6''), 6.74 (d, 1H, H-2, $J_{1,2} = 16.2$ Hz), 3.02 (bs, A_2B_2 , 4H, CH_2CH_2) ppm; ^{13}C NMR (100 MHz, $CDCl_3$): d 199.6 (C-3), 143.0 (C-1), 141.5 (C-1''), 134.7 (C-1'), 130.7 (C-4^a), 129.2 (C-2'/6^b), 128.8 (C-3'/5^b), 128.6 (C-2''/6^{bb}), 128.5 (C-3''/5^{bb}), 126.4 (C-4''/2^a), 42.7 (C-4), 30.4 (C-5) ppm; Anal. Calcd. for $C_{17}H_{16}O$ (MW 236.31): C, 86.40; H, 6.82%. Found: C, 86.01; H, 6.90%. HR-ESI-MS: $[M + H]^+$ 237.1295; calc. 237.1279.

The 1H NMR and ^{13}C NMR data of compound **5a** were in good agreement with the data given in the literature [37].

4.2. (E)-1-(4-hydroxyphenyl)-5-phenylpent-1-en-3-one (5b)

The synthetic procedure described above for **5a** was applied using 4-phenyl-2-butanone (**6**) and 4-hydroxybenzaldehyde (**9**) as a reagent and Et₂O as a solvent for 60 h to give **5b** in a yield of 31%. Chromatography was performed using EtOAc/hexanes at a ratio of 20:80. R_f (AcOEt/hexanes 3:7): 0.8. Light yellow solid. Mp 136–137 °C. Anal. Calcd. for C₁₇H₁₆O₂ (MW 252.31): C, 80.93; H, 6.39%. Found: C, 80.79; H, 6.51%. HR-ESI-MS: [M + H]⁺ 253.1250; calc. 253.1228.

4.3. (E)-1-(4-methoxyphenyl)-5-phenylpent-1-en-3-one (5c)

The synthetic procedure described above for **5a** was applied using 4-phenyl-2-butanone (**6**) and 4-methoxybenzaldehyde (**10**) as a reagent and Et₂O as a solvent for 48 h to give **5c** in a yield of 72%. Chromatography was performed using EtOAc/hexanes in a ratio of 4:96. R_f (AcOEt/hexanes 1:9): 0.6. White solid. Mp 95–96 °C; Anal. Calcd. for C₁₈H₁₈O₂ (MW 266.34): C, 81.17; H, 6.81%. Found: C, 81.10; H, 6.87%. HR-ESI-MS: [M + H]⁺ 267.1398; calc. 267.1385.

The ¹H NMR and ¹³C NMR data of compound **5c** were in good agreement with the data given in the literature [38].

4.4. (E)-1-(4-hydroxy-3-methoxyphenyl)-5-phenylpent-1-en-3-one (5d)

The synthetic procedure described above for **5a** was applied using 4-phenyl-2-butanone (**6**) and 4-hydroxy-3-methoxybenzaldehyde (**11**) as a reagent and Et₂O as a solvent for 48 h to give **5d** in a yield of 61%. Chromatography was performed using EtOAc/hexanes in a ratio of 20:80. R_f (AcOEt/hexanes 3:7): 0.7. Yellow solid. Mp 89–90 °C. Anal. Calcd. for C₁₈H₁₈O₃ (MW 282.34): C, 76.57; H, 6.43%. Found: C, 76.11; H, 6.57%. HR-ESI-MS: [M + H]⁺ 283.1353; calc. 283.1334.

The ¹H NMR and ¹³C NMR data of compound **5d** were in good agreement with the data given in the literature [39].

4.5. (E)-1-(3-hydroxy-4-methoxyphenyl)-5-phenylpent-1-en-3-one (5e)

The synthetic procedure described above for **5a** was applied using 4-phenyl-2-butanone (**6**) and 3-hydroxy-4-methoxybenzaldehyde (**12**) as a reagent and Et₂O as a solvent for 48 h to give **5e** in a yield of 44%. Chromatography was performed using EtOAc/hexanes in a ratio of 20:80. R_f (AcOEt/hexanes 3:7): 0.6. Brown solid. Mp 94–95 °C. Anal. Calcd. for C₁₈H₁₈O₃ (MW 282.34): C, 76.57; H, 6.43%. Found: C, 76.77; H, 6.42%. HR-ESI-MS: [M + H]⁺ 283.1354; calc. 283.1334.

4.6. (E)-1-(3,4-dihydroxyphenyl)-5-phenylpent-1-en-3-one (5f) [40]

The synthetic procedure described above for **5a** was applied using 4-phenyl-2-butanone (**6**) and 3,4-dihydroxybenzaldehyde (**13**) as a reagent and THF as a solvent for 48 h to give **5f** in a yield of 53%. Chromatography was performed using EtOAc/hexanes in a ratio of 30:70. R_f (AcOEt/hexanes 3:7): 0.6. Brown solid. Mp 167–168 °C. Anal. Calcd. for C₁₇H₁₆O₃ (MW 268.31): C, 76.10; H, 6.01%. Found: C, 75.99; H, 6.17%. HR-ESI-MS: [M + H]⁺ 269.1193; calc. 269.1177.

4.7. (E)-5-(4-hydroxyphenyl)-1-phenylpent-1-en-3-one (5g)

The synthetic procedure described above for **5a** was applied using 4-hydroxyphenyl-2-butanone (**7**) and benzaldehyde (**8**) as a reagent and Et₂O as a solvent for 48 h to give **5g** in a yield of 37%. Chromatography was performed using EtOAc/hexanes in a ratio of 15:85. R_f (AcOEt/hexanes 2:8): 0.6. Light yellow solid. Mp 96–97 °C. Anal. Calcd. for C₁₇H₁₆O₂ (MW 252.31): C, 80.93; H, 6.39%. Found: C, 81.23; H, 6.54%. HR-ESI-MS: [M + H]⁺ 253.1243; calc. 253.1228.

4.8. (E) 1,5-bis(4-hydroxyphenyl)pent-1-en-3-one (5h)

The synthetic procedure described above for **5a** was applied using 4-hydroxyphenyl-2-butanone (**7**) and 4-hydroxybenzaldehyde (**9**) as a reagent and THF as a solvent for 48 h to give **5h** in a yield of 20%. Chromatography was performed using EtOAc/hexanes in a ratio of 25:75. R_f (AcOEt/hexanes 3:7): 0.46. Yellow solid. Mp 146–147 °C. Anal. Calcd. for C₁₇H₁₆O₃ (MW 268.31): C, 76.10; H, 6.01%. Found: C, 76.00; H, 6.19%. HR-ESI-MS: [M + H]⁺ 269.1175; calc. 269.1177.

4.9. (E)-5-(4-hydroxyphenyl)-1-(4-methoxyphenyl)pent-1-en-3-one (5i)

The synthetic procedure described above for **5a** was applied using 4-hydroxyphenyl-2-butanone (**7**) and 4-methoxybenzaldehyde (**10**) as a reagent and THF as a solvent for 48 h to give **5i** in a yield of 36%. Chromatography was performed using EtOAc/hexanes in a ratio of 20:80. R_f (AcOEt/hexanes 3:7): 0.6. Light yellow solid. Mp 83–84 °C. Anal. Calcd. for C₁₈H₁₈O₃·0.4 H₂O (MW 289.54): C, 74.6; H, 6.59%. Found: C, 74.11; H, 6.42%. HR-ESI-MS: [M + H]⁺ 283.1350; calc. 283.1334.

4.10. (E)-1-(4-hydroxy-3-methoxyphenyl)-5-(4-hydroxyphenyl)pent-1-en-3-one (5j)

The synthetic procedure described above for **5a** was applied using 4-hydroxyphenyl-2-butanone (**7**) and 4-hydroxy-3-methoxybenzaldehyde (**11**) as a reagent and THF as a solvent for 48 h to give **5j** in a yield of 21%. Chromatography was performed using EtOAc/hexanes in a ratio of 30:70. R_f (AcOEt/hexanes 4:6): 0.75. Yellow solid. Mp 131–132 °C. Anal. Calcd. for C₁₈H₁₈O₄ (MW 298.34): C, 72.47; H, 6.08%. Found: C, 72.06; H, 6.08%. HR-ESI-MS: [M + H]⁺ 299.1303; calc. 299.1283.

4.11. (E)-1-(3-hydroxy-4-methoxyphenyl)-5-(4-hydroxyphenyl)pent-1-en-3-one (5k)

The synthetic procedure described above for **5a** was applied using 4-hydroxyphenyl-2-butanone (**7**) and 3-hydroxy-4-methoxybenzaldehyde (**12**) as a reagent and THF as a solvent for 48 h to give **5k** in a yield of 11%. Chromatography was performed using EtOAc/hexanes in a ratio of 1:1. R_f (AcOEt/hexanes 4:6): 0.7. Light yellow solid. Mp 130–131 °C. Anal. Calcd. for $C_{18}H_{18}O_4$ (MW 298.34): C, 72.47; H, 6.08%. Found: C, 72.42; H, 5.89%. HR-ESI-MS: $[M + H]^+$ 299.1264; calc. 299.1283.

4.12. (E)-1-(3,4-dihydroxyphenyl)-5-(4-hydroxyphenyl)pent-1-en-3-one (5l)

The synthetic procedure described above for **5a** was applied using 4-hydroxyphenyl-2-butanone (**7**) and 3,4-dihydroxybenzaldehyde (**13**) as a reagent and THF as a solvent for 48 h to give **5l** in a yield of 23%. Chromatography was performed using EtOAc/hexanes in a ratio of 40:60. R_f (AcOEt/hexanes 5:5): 0.5. Yellow solid. Mp 202–203 °C. Anal. Calcd. for $C_{17}H_{16}O_4$ (MW 284.31): C, 71.82; H, 5.67%. Found: C, 71.52; H, 5.99%. HR-ESI-MS: $[M + H]^+$ 285.1140; calc. 285.1126.

The 1H NMR and ^{13}C NMR spectra of compounds **5a–5l** are given in the supplementary material file as graphical and numerical data.

4.13. Cytotoxicity testing**4.13.1. Cell lines and culture conditions**

Human GBM (U87-MG), breast cancer (MCF-7), prostate cancer (PC-3), and pulmonary alveolar epithelial cells (HPAEpiC) cell lines from the American Type Culture Collection (ATCC) were used for the cytotoxicity testing of compounds **5a–5l**. The cells were grown as a single layer in appropriate medium containing 10% FBS, 1% penicillin/streptomycin, and 1% L-glutamine at 37 °C and 5% CO_2 atmosphere.

4.13.2. MTT assay

The cytotoxicity analyses of all of the compounds were investigated by determining cell viability based on the colorimetric MTT assay, which was conducted according to the manufacturer's guide. First, 2×10^5 cells/well were seeded in a 96-well plate and then incubated at 37 °C in a 5% CO_2 environment for 24 h. The medium was aspirated the following day, and 100 mL of each concentration of the 12 tested compounds (3.125, 6.25, 12.5, 25, 50, and 100 mg/L) were separately added to each well. The plates were then incubated for 48 h at 37 °C with 5% CO_2 . Next, 10 μ L of MTT solution was added to each well and the plate was incubated for 4 h. The culture medium was aspirated from the wells without dispersing the cell layer and then 100 μ L of DMSO was added to each well and stirred on an orbital stirrer to dissolve the formazan crystals. Each sample was read at a wavelength of 570 nm in a spectrophotometer and absorbance values were obtained. A wavelength of 630 nm was used as the reference. Cell viability was expressed as a percentage compared to the untreated cells. All experiments were performed in triplicate [41,42].

4.13.3. Hoechst 33258 staining

Hoechst 33258 staining was used to assess significant morphological changes in the nuclear chromatin of the cells. Briefly, the cells were seeded on coverslips in a 6-well plate and treated with the IC_{50} concentration of compounds **5a** and **5i**. After 48 h, the cover glasses were washed carefully with PBS, fixed in 4% paraformaldehyde in 0.01 M PBS for 1 h, and washed twice with PBS. The cells were then stained with 20 μ g/mL Hoechst 33258 for 10 min. Thereafter, the cells were observed using a Leica DMIRB fluorescence microscope (Leica Microsystems, Wetzlar, Germany). Additionally, 100 μ M H_2O_2 was used as a positive control.

4.13.4. Statistical analysis

IBM SPSS Statistics 20.0 for Windows (IBM Corp., Armonk, NY, USA) was used for statistical analyses and two-way ANOVA was used to statistically compare data from multiple groups. $P < 0.05$ was considered statistically significant.

Acknowledgments

This work was a part of the PhD dissertation of Neslihan Çelebioğlu, who expresses her thanks to the Scientific and Technological Research Council of Türkiye (TÜBİTAK) for supporting her through a project fellowship (Grant Numbers: 113Z197 and 116Z827). The authors particularly thank Atatürk University for its financial support of this work (Grant Number: BAP 116Z827).

References

- [1] Claeson P, Tuchinda P, Reutrakul V. Naturally occurring 1,7-diarylheptanoids. *Journal of the Indian Chemical Society* 1994; 71 (6-8): 509-521.
- [2] Claeson P, Claseon UP, Tuchinda P, Reutrakul V. Occurrence, structure and bioactivity of 1,7-diarylheptanoids. *Studies in Natural Products Chemistry* 2002; 26: 881-905. [https://doi.org/10.1016/S1572-5995\(02\)80021-7](https://doi.org/10.1016/S1572-5995(02)80021-7)
- [3] Keserü GM, Nogradi M. The chemistry of natural diarylheptanoids. *Studies in Natural Products Chemistry* 1995; 17: 357-394. [https://doi.org/10.1016/S1572-5995\(05\)80090-0](https://doi.org/10.1016/S1572-5995(05)80090-0)
- [4] Lv H, She G. Naturally occurring diarylheptanoids. *Natural Product Communications* 2010; 5 (10): 1687-1708. <https://doi.org/10.1177/1934578X1000501035>
- [5] Mirzaei H, Shakeri A, Rashidi B, Jalili A, Banikazemi Z et al. Phytosomal curcumin: a review of pharmacokinetic, experimental and clinical studies. *Biomedicine & Pharmacotherapy* 2017; 85: 102-112. <https://doi.org/10.1016/j.biopha.2016.11.098>
- [6] Celebioglu N, Ozgen U, Secen H. Naturally occurring 1,5-diarylpentanoids: a review. *Organic Communications* 2017; 10 (4): 250-258. <https://doi.org/10.25135/acg.oc.33.17.10.052>
- [7] Goel A, Kunnumakkara AB, Aggarwal BB. Curcumin as “curecumin”: from kitchen to clinic. *Biochemical Pharmacology* 2008; 75: 787-809. <https://doi.org/10.1016/j.bcp.2007.08.016>
- [8] Anand P, Thomas SG, Kunnumakkara AB, Sundaram C, Harikumar KB et al. Biological activities of curcumin and its analogues (congeners) made by man and mother nature. *Biochemical Pharmacology* 2008; 76: 1590-1611. <https://doi.org/10.1016/j.bcp.2008.08.008>
- [9] Anand P, Sundaram C, Jhurani S, Kunnumakkara AB, Aggarwal BB. Curcumin and cancer: an “old-age” disease with an “age-old” solution. *Cancer Letters* 2008; 267: 133-164. <https://doi.org/10.1016/j.canlet.2008.03.025>
- [10] Aggarwal BB, Harikumar KB. Potential therapeutic effects of curcumin, the anti-inflammatory agent, against neurodegenerative, cardiovascular, pulmonary, metabolic, autoimmune and neoplastic diseases. *International Journal of Biochemistry & Cell Biology* 2009; 41: 40-59. <https://doi.org/10.1016/j.biocel.2008.06.010>
- [11] Agrawal DK, Mishra PK. Curcumin and its analogues: potential anticancer agents. *Medicinal Research Reviews* 2010; 30: 818-860. <https://doi.org/10.1002/med.20188>
- [12] Moreira J, Saraiva L, Pinto MM, Cidade H. Diarylpentanoids with antitumor activity: a critical review of structure-activity relationship studies. *European Journal of Medicinal Chemistry* 2020; 192: 112177. <https://doi.org/10.1016/j.ejmech.2020.112177>
- [13] Leong SW, Chia SL, Abas F, Yusoff K. Synthesis and in-vitro anti-cancer evaluations of multi-methoxylated asymmetrical diarylpentanoids as intrinsic apoptosis inducer against colorectal cancer. *Bioorganic & Medicinal Chemistry Letters* 2020; 30 (8): 127065. <https://doi.org/10.1016/j.bmcl.2020.127065>
- [14] Wang L, Cheng L, Ma L, Farooqi AA, Qiao G et al. Alnustone inhibits the growth of hepatocellular carcinoma via ROS-mediated PI3K/Akt/mTOR/p70S6K Axis. *Phytotherapy Research* 2022; 36 (1): 525-542. <https://doi.org/10.1002/ptr.7337>
- [15] Kucukoglu K, Secinti H, Ozgur A, Secen H, Tutar Y. Synthesis, molecular docking, and antitumoral activity of alnustone-like compounds against estrogen receptor alpha-positive human breast cancer. *Turkish Journal of Chemistry* 2015; 39 (1): 179-193. <https://doi.org/10.3906/KIM-1408-72>
- [16] Nyandoro SS, Joseph CC, Nkunya HHM, Hosea MMK. New antimicrobial, mosquito larvicidal and other metabolites from two *Artabotrys* species. *Natural Product Research* 2013; 27 (16): 1450-1458. <https://doi.org/10.1080/14786419.2012.725397>
- [17] Gao K, Tang HF, Lu YY, Wang XY, Zhang W et al. Chemical constituents in fruits of *Lycium barbarum* L. *Zhongnan Yaoxue* 2014; 12: 324-327. <https://doi.org/10.3390/molecules24081585>
- [18] Chen J, McKay RM, Parada LF. Malignant glioma: lessons from genomics, mouse models, and stem cells. *Cell* 2012; 149 (1): 36-47. <https://doi.org/10.1016/j.cell.2012.03.009>
- [19] Cancer.Net Editorial Board. *Brain Tumor: Statistics 2016*. Alexandria, VA, USA: American Society of Clinical Oncology, 2016. Available at <https://www.cancer.net/cancer-types/brain-tumor/statistics>
- [20] Louis DN, Perry A, Reifenberger G, von Deimling A, Figarella-Branger D et al. The 2016 World Health Organization Classification of Tumors of the Central Nervous System: A summary. *Acta Neuropathologica* 2016; 131 (6): 803-820. <https://doi.org/10.1007/s00401-016-1545-1>
- [21] Hanif F, Muzaffar K, Perveen K, Malhi SM, Simjee SU. Glioblastoma multiforme: a review of its epidemiology and pathogenesis through clinical presentation and treatment. *Asian Pacific Journal of Cancer Prevention* 2017; 18 (1): 3-9. <https://doi.org/10.22034/APJCP.2017.18.1.3>
- [22] Tamimi AF, Juweid M. Epidemiology and outcome of glioblastoma. In: Vleeschouwer SD (editor). *Epidemiology of Glioblastoma*. Brisbane, Australia: Codon Publications, 2017, pp. 143-153. <https://doi.org/10.15586/codon.glioblastoma.2017.ch8>
- [23] Li K, Lu D, Guo Y, Wang C, Liu X et al. Trends and patterns of incidence of diffuse glioma in adults in the United States, 1973-2014. *Cancer Medicine* 2018; 7 (10): 5281-5290. <https://doi.org/10.1002/cam4.1757>

- [24] Behl T, Sharma A, Sharma L, Sehgal A, Singh S et al. Current perspective on the natural compounds and drug delivery techniques in glioblastoma multiforme. *Cancers* 2021; 13 (11): 2765. <https://doi.org/10.3390/cancers13112765>
- [25] Yi M, Li T, Niu M, Luo S, Chu Q et al. Epidemiological trends of women's cancers from 1990 to 2019 at the global, regional, and national levels: a population-based study. *Biomarker Research* 2021; 9: 55. <https://doi.org/10.1186/s40364-021-00310-y>
- [26] Sung H, Ferlay J, Siegel RL, Laversanne M, Soerjomataram I et al. Global Cancer Statistics 2020: GLOBOCAN estimates of incidence and mortality worldwide for 36 cancers in 185 countries. *CA Cancer Journal for Clinicians* 2021; 71 (3): 209-249. <https://doi.org/10.3322/caac.21660>
- [27] Heer E, Harper A, Escandor N, Sung H, McCormack V et al. Global burden and trends in premenopausal and postmenopausal breast cancer: a population-based study. *Lancet Global Health* 2020; 8: e1028. [https://doi.org/10.1016/S2214-109X\(20\)30215-1](https://doi.org/10.1016/S2214-109X(20)30215-1)
- [28] Rebello RJ, Oing C, Knudsen KE, Loeb S, Johnson DC et al. Prostate cancer. *Nature Reviews Disease Primers* 2021; 7: 9. <https://doi.org/10.1038/s41572-020-00243-0>
- [29] Göksu S, Çelik H, Seçen H. An efficient synthesis of alnustone, a naturally occurring compound. *Turkish Journal of Chemistry* 2003; 27: 31-34.
- [30] Demir ŞB, Seçinti H, Çelebioğlu N, Özdal M, Sezen A et al. Syntheses and antibacterial activities of 4 linear nonphenolic diarylheptanoids. *Turkish Journal of Chemistry* 2020; 4 (3): 589-601. <https://doi.org/10.3906/kim-1911-61>
- [31] Burmaoglu S, Celik H, Göksu S, Maraş A, Altundaş R et al. Synthesis of two alnustone-like natural diarylheptanoids via C₄+C₃ strategy. *Synthesis Communications* 2009; 39: 1549-1562. <https://doi.org/10.1080/00397910802542036>
- [32] Castro E, Moreira J, Silva PMA, Saraiva L, Pinto M et al. Biological evaluation of new diarylpentanoic acid analogues for antitumor activity (Proceeding abstract). *Scientific Letters* 2023; 1 (Suppl. 1): 26. <https://doi.org/10.48797/sl.2023.26>
- [33] Leong SW, Chia SL, Abas F, Yusoff K. Synthesis and in-vitro anti-cancer evaluations of multi-methoxylated asymmetrical diarylpentanoic acids as intrinsic apoptosis inducer against colorectal cancer. *Bioorganic & Medicinal Chemistry Letters* 2020; 30 (8): 127065. <https://doi.org/10.1016/j.bmcl.2020.127065>
- [34] Paulraj F, Abas F, Lajis NH, Othman I, Naidu R. Molecular pathways modulated by curcumin analogue, diarylpentanoic acids in cancer. *Biomolecules* 2019; 9 (7): 270. <https://doi.org/10.3390/biom9070270>
- [35] López-Lázaro M. Two preclinical tests to evaluate anticancer activity and to help validate drug candidates for clinical trials. *Oncoscience* 2015; 2 (2): 91-98. <https://doi.org/10.18632/oncoscience.132>
- [36] López-Lázaro M. How many times should we screen a chemical library to discover an anticancer drug? *Drug Discovery Today* 2015; 20 (2): 167-169. <https://doi.org/10.1016/j.drudis.2014.12.006>
- [37] Li W, Wu XF. Ruthenium-catalyzed conjugate hydrogenation of α,β -enones by in situ generated dihydrogen paraformaldehyde and water. *European Journal of Organic Chemistry* 2015; 20: 331-335. <https://doi.org/10.1002/ejoc.201403359>
- [38] Lao Z, Zhang H, Toy PH. Reductive halogenation reactions: selective synthesis of unsymmetrical α -haloketones. *Organic Letters* 2019; 21: 8149-8152. <https://doi.org/10.1021/acs.orglett.9b02324>
- [39] Oh S, Jang S, Kim D, Han IO, Jung JC. Synthesis and evaluation of biological properties of benzylideneacetophenone derivatives. *Archives of Pharmacal Research* 2006; 29 (6): 469-475. <https://doi.org/10.1007/BF02969418>
- [40] Doiron JA, Leblanc LM, Hebert MJG, Levesque NA, Pare AF et al. Structure-activity relationship of caffeic acid phenethyl ester analogs as new 5-lipoxygenase inhibitors. *Chemical Biology & Drug Design* 2017; 89 (4): 514-528. <https://doi.org/10.1111/cbdd.12874>
- [41] Özdemir Ö, Marinelli L, Cacciatore I, Ciulla M, Emsen B et al. Anticancer effects of novel NSAIDs derivatives on cultured human glioblastoma cells. *Zeitschrift für Naturforschung C* 2020; 76 (7-8): 329-335. <https://doi.org/10.1515/znc-2020-0093>
- [42] Özgeriş B, Akbaba Y, Özdemir Ö, Türkez H, Göksu S. Synthesis and anticancer activity of novel ureas and sulfamides incorporating 1-aminotetralins. *Archives of Medical Research* 2007; 48 (6): 513-519. <https://doi.org/10.1016/j.arcm.2017.12.002>

Supplementary Material

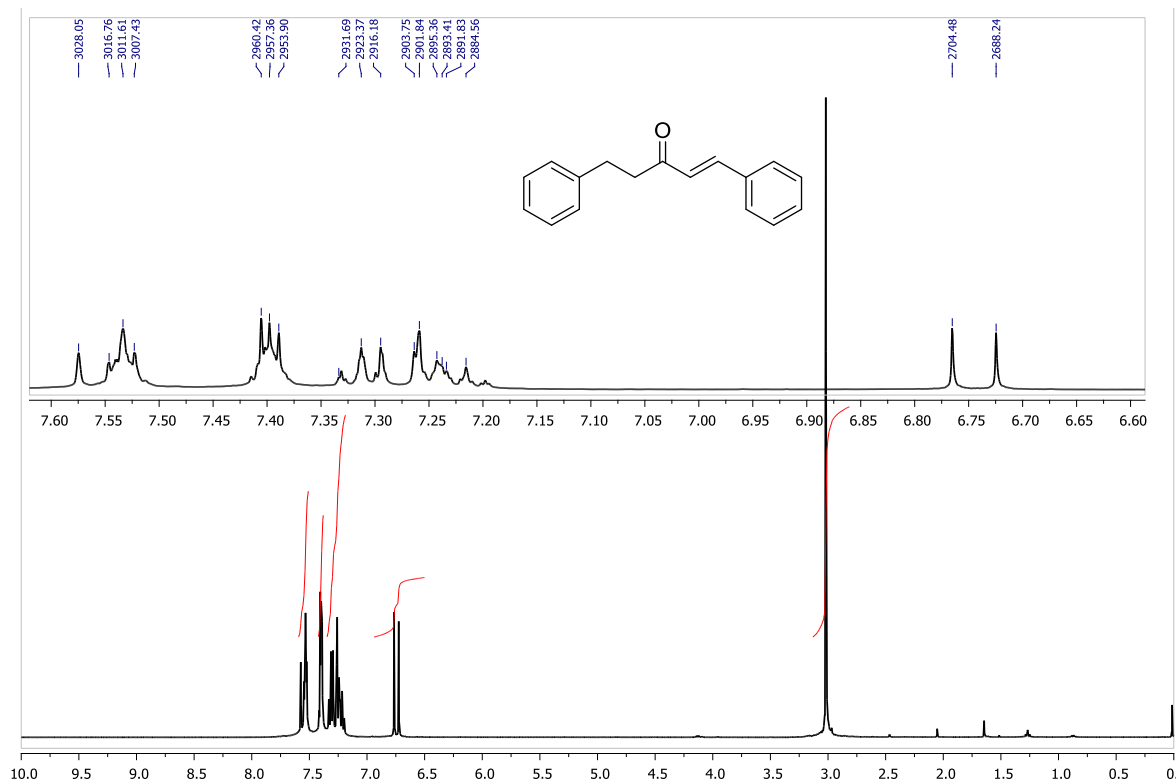


Figure 1. ¹H-NMR spectrum of (*E*)-1,5-diphenylpent-1-en-3-one (5a) (CDCl₃).

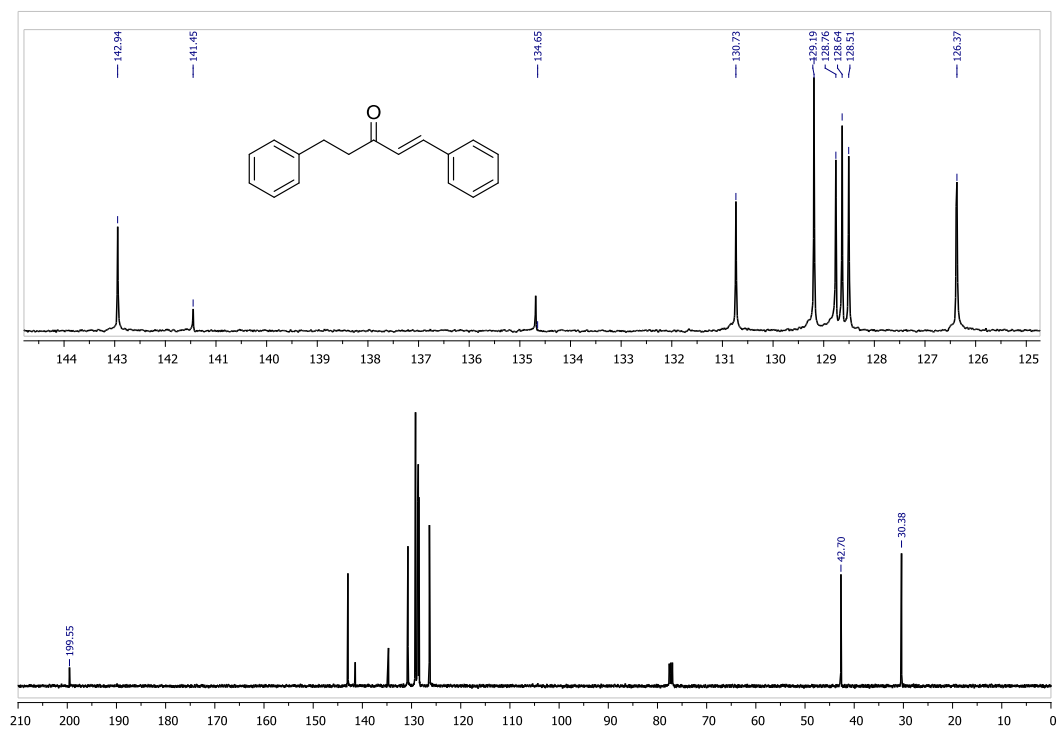


Figure 2. ¹³C-NMR spectrum of (*E*)-1,5-diphenylpent-1-en-3-one (5a) (CDCl₃).

User Spectra

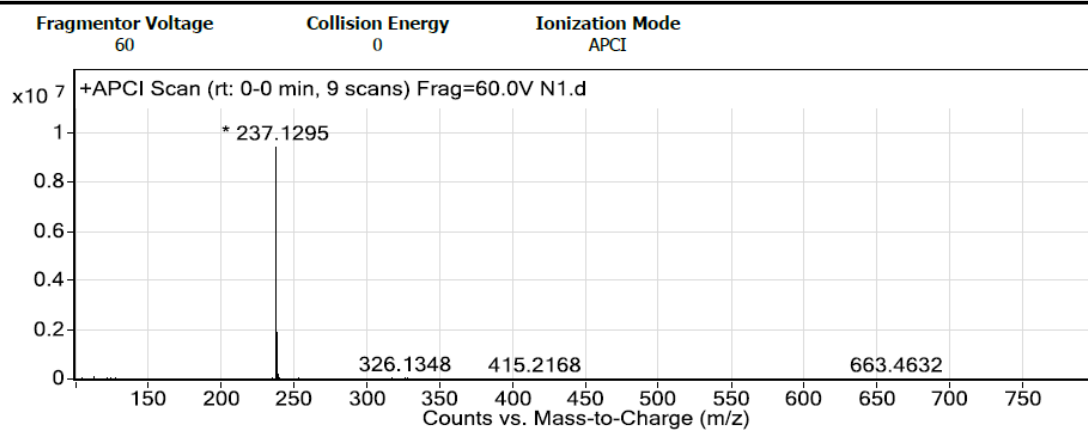


Figure 3. HRMS spectrum of (*E*)-1,5-diphenylpent-1-en-3-one (**5a**). ($C_{17}H_{16}O+H$)⁺, Calc: 237.1279.

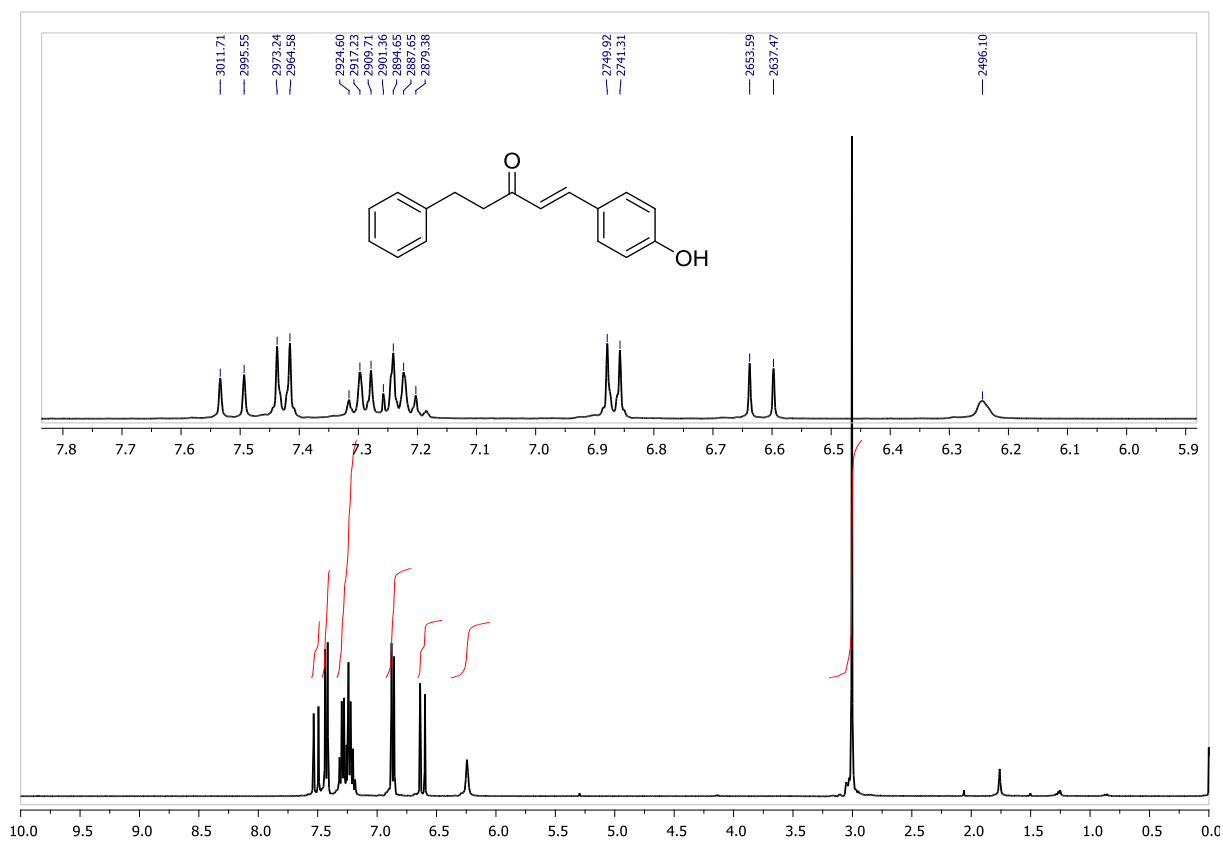


Figure 4. ¹H-NMR spectrum of (*E*)-1-(4-hydroxyphenyl)-5-phenylpent-1-en-3-one (**5b**) (CDCl₃).

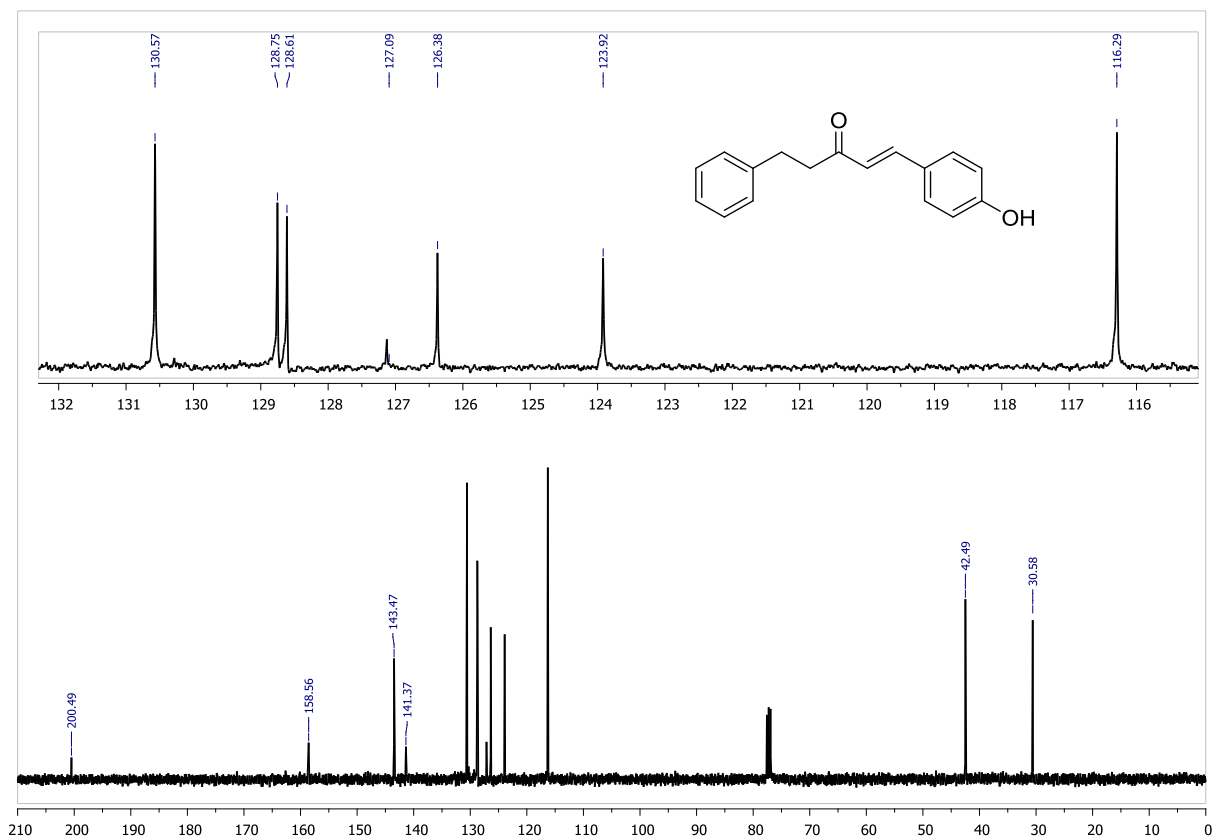


Figure 5. ^{13}C -NMR spectrum of *(E)*-1-(4-hydroxyphenyl)-5-phenylpent-1-en-3-one (5b) (CDCl_3).

User Spectra

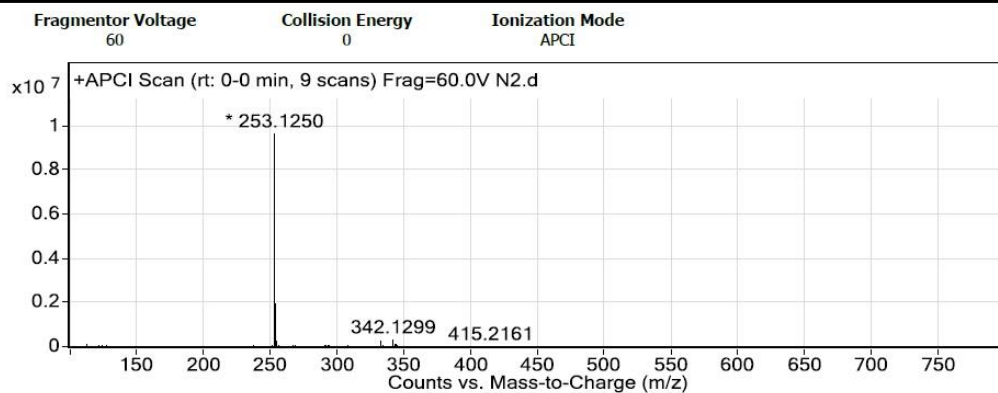


Figure 6. HRMS spectrum of *(E)*-1-(4-hydroxyphenyl)-5-phenylpent-1-en-3-one (5b). $(\text{C}_{17}\text{H}_{16}\text{O}_2+\text{H})^+$, Calc: 253.1228.

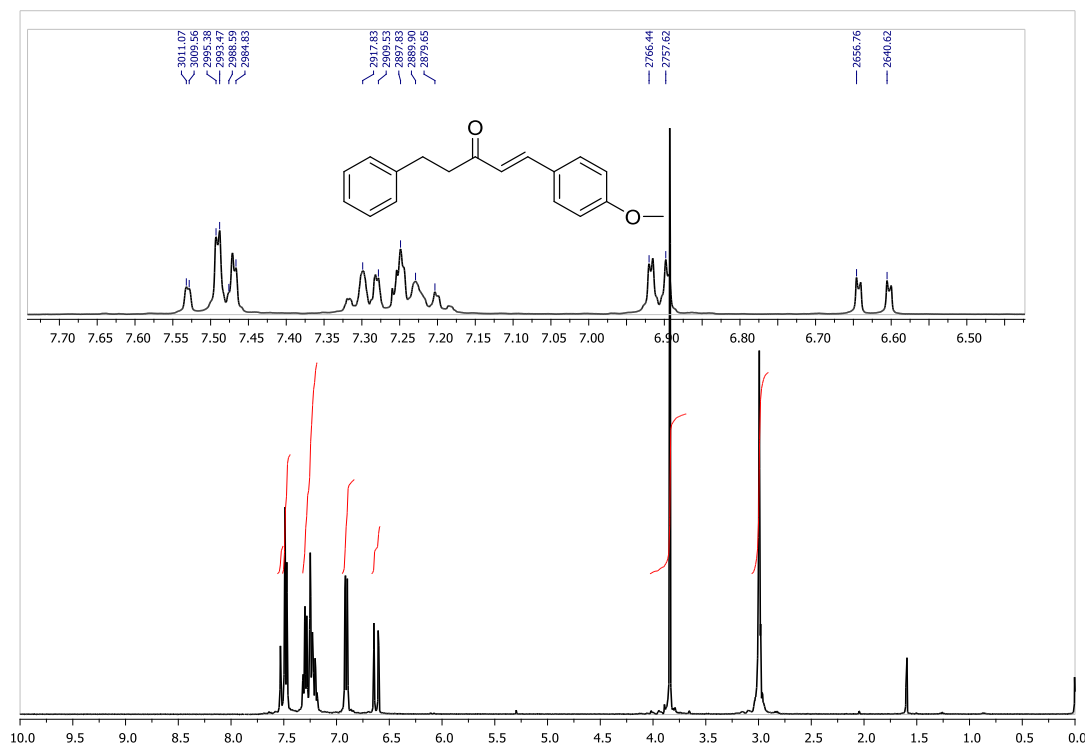


Figure 7. ¹H-NMR spectrum of (*E*)-1-(4-methoxyphenyl)-5-phenylpent-1-en-3-one (5c) (CDCl₃).

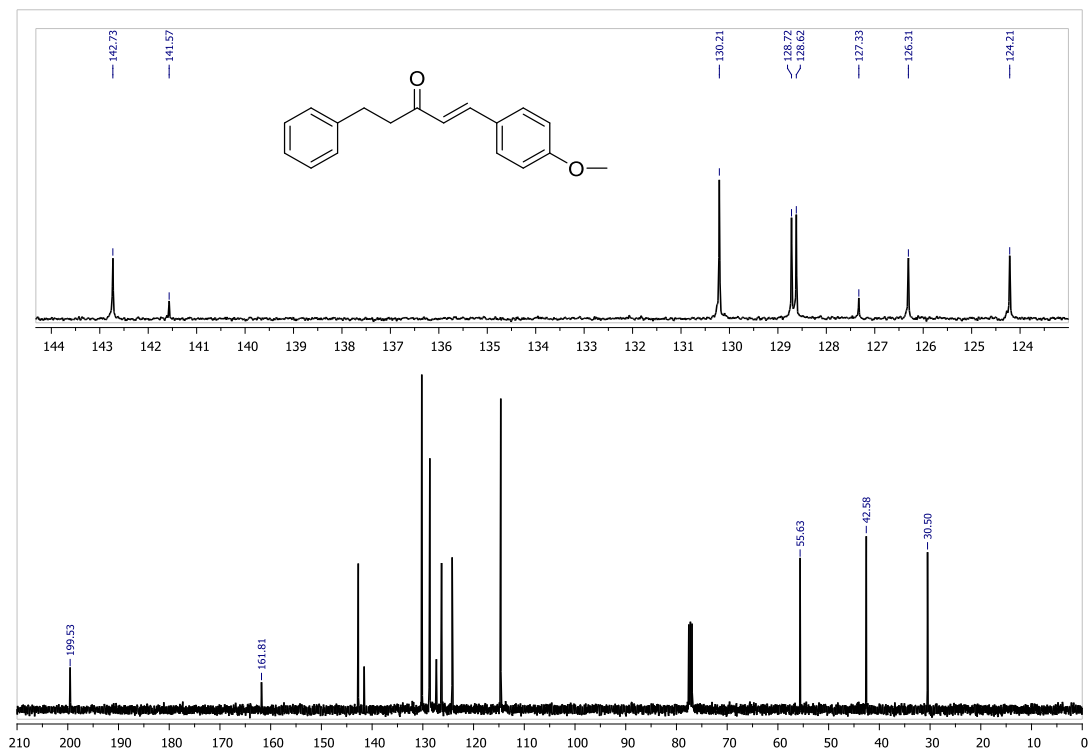


Figure 8. ¹³C-NMR spectrum of (*E*)-1-(4-methoxyphenyl)-5-phenylpent-1-en-3-one (5c) (CDCl₃).

User Spectra

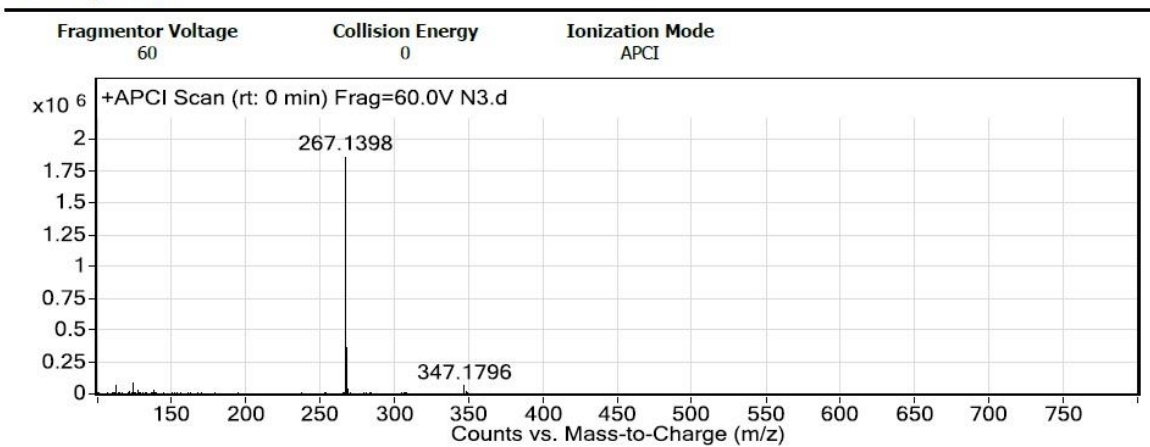


Figure 9. HRMS spectrum of (*E*)-1-(4-methoxyphenyl)-5-phenylpent-1-en-3-one (**5c**). ($C_{18}H_{18}O_2+H$)⁺, Calc: 267.1385.

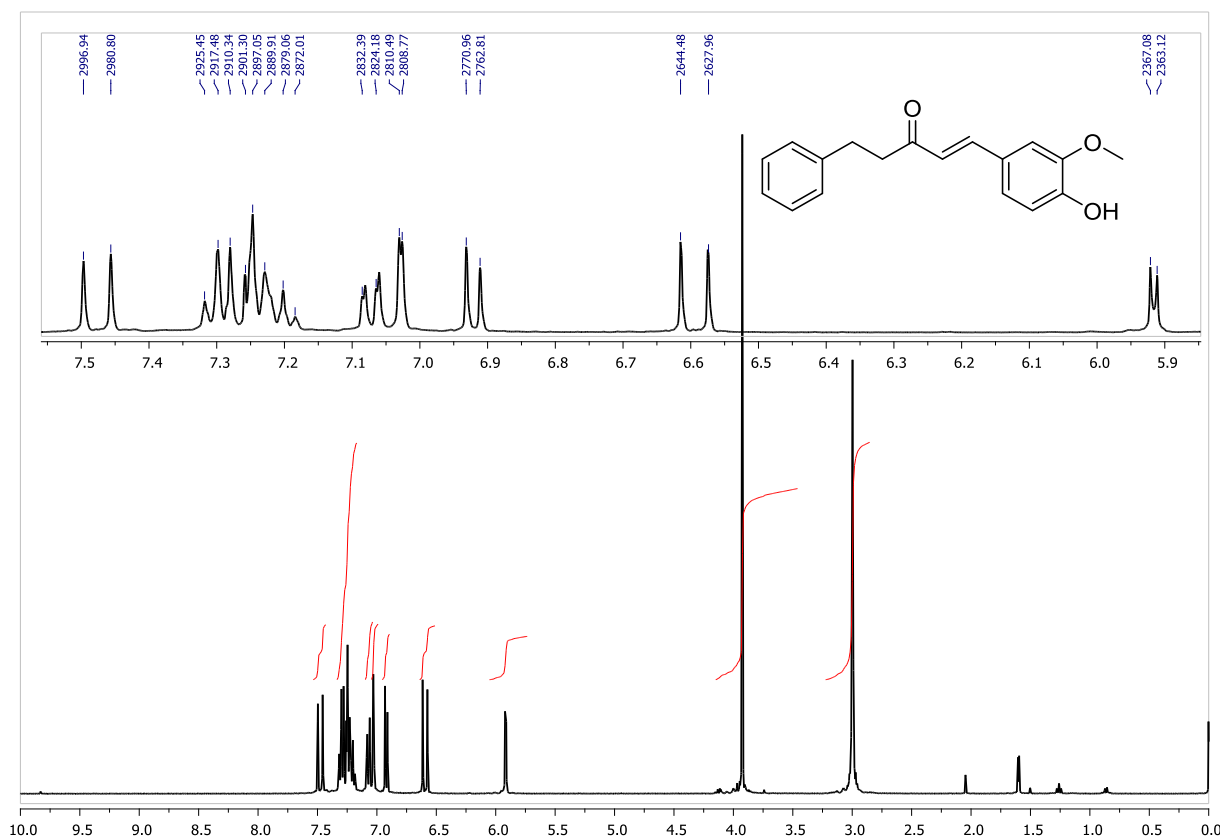


Figure 10. ¹H-NMR spectrum of (*E*)-1-(4-hydroxy-3-methoxyphenyl)-5-phenylpent-1-en-3-one (**5d**) ($CDCl_3$).

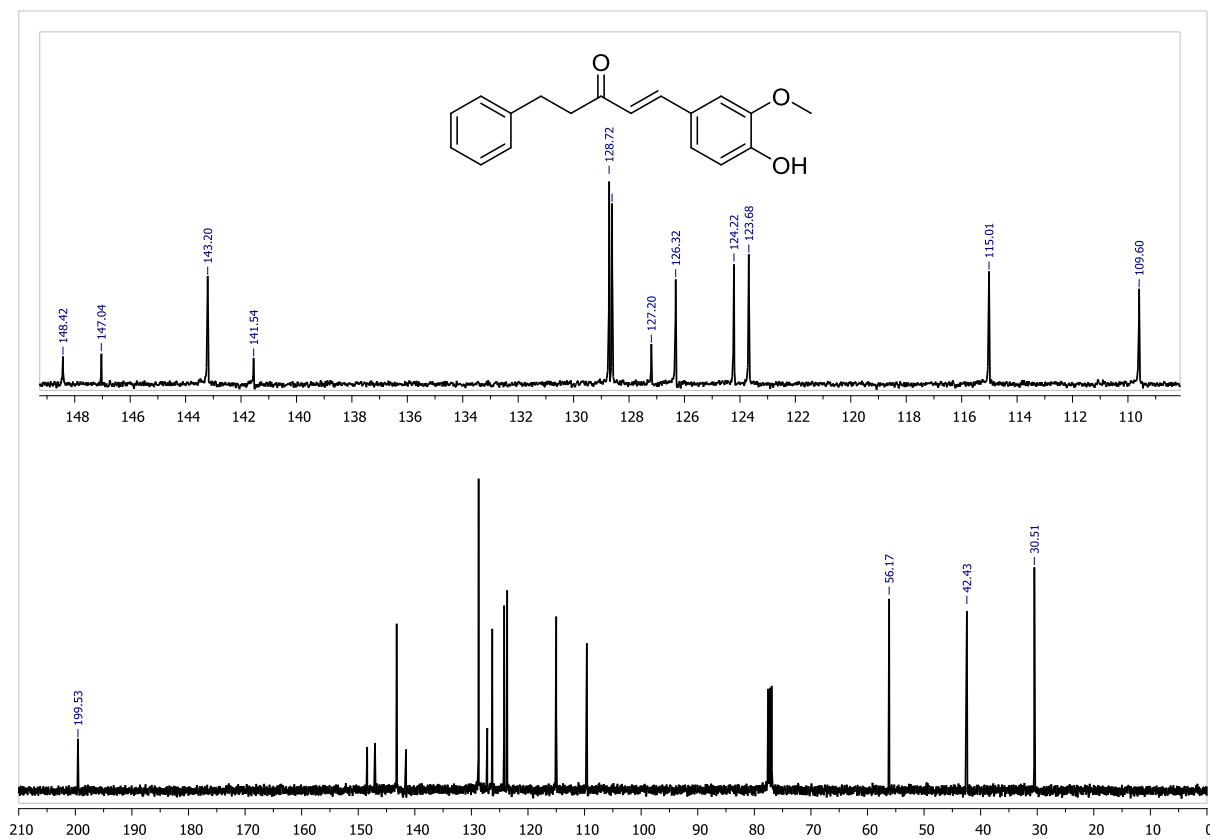


Figure 11. ^{13}C -NMR spectrum of (*E*)-1-(4-hydroxy-3-methoxyphenyl)-5-phenylpent-1-en-3-one (**5d**) (CDCl_3).

User Spectra

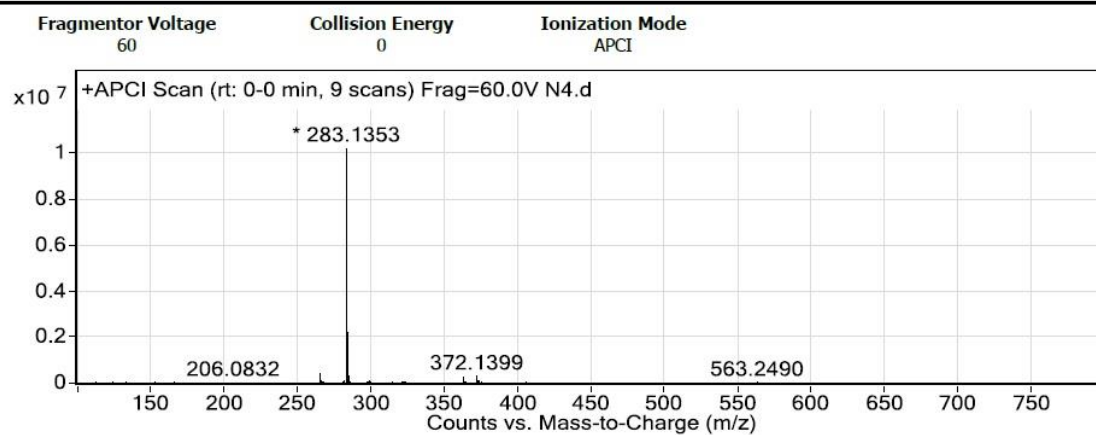


Figure 12. HRMS spectrum of (*E*)-1-(4-hydroxy-3-methoxyphenyl)-5-phenylpent-1-en-3-one (**5d**). ($\text{C}_{18}\text{H}_{18}\text{O}_3+\text{H}$) $^+$, Calc: 283.1334.

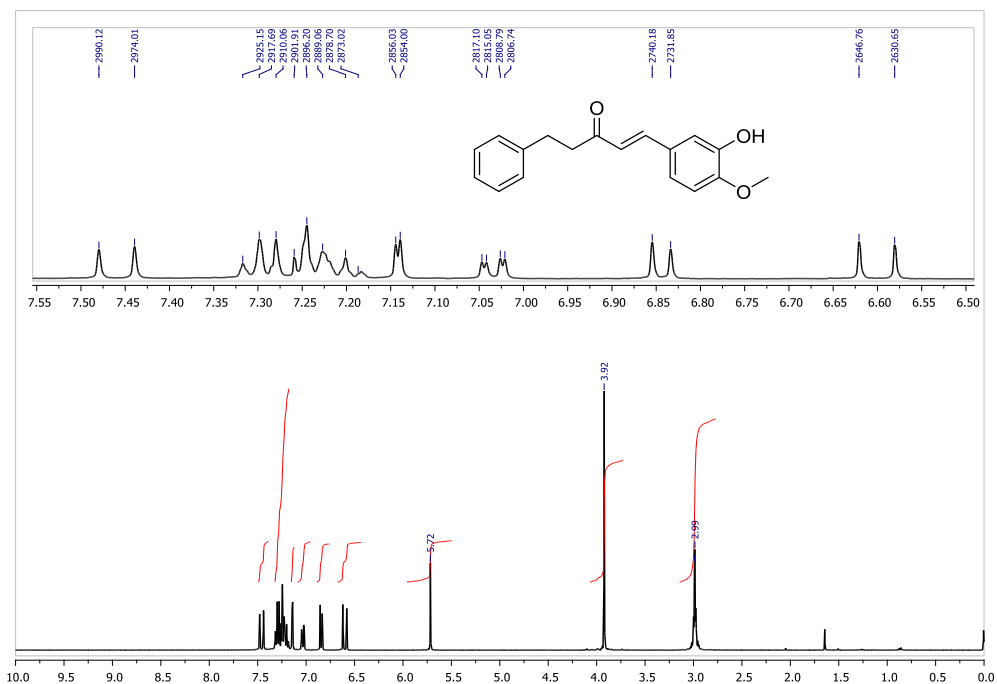


Figure 13. ¹H-NMR spectrum of (E)-1-(3-hydroxy-4-methoxyphenyl)-5-phenylpent-1-en-3-one (5e) (CDCl₃).

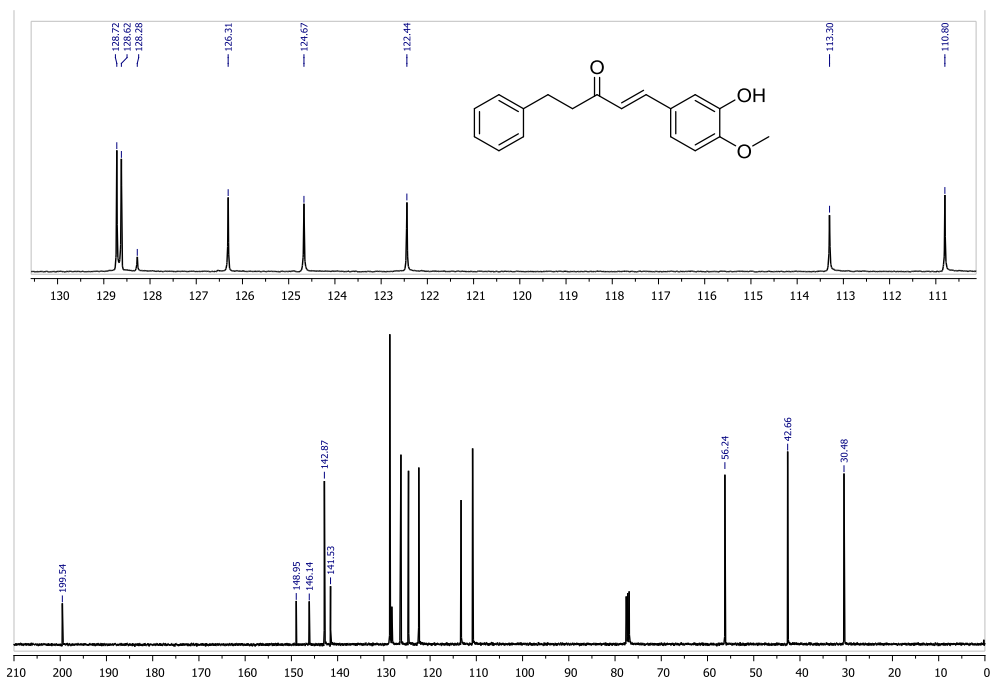


Figure 14. ¹³C-NMR spectrum of (E)-1-(3-hydroxy-4-methoxyphenyl)-5-phenylpent-1-en-3-one (5e) (CDCl₃).

User Spectra

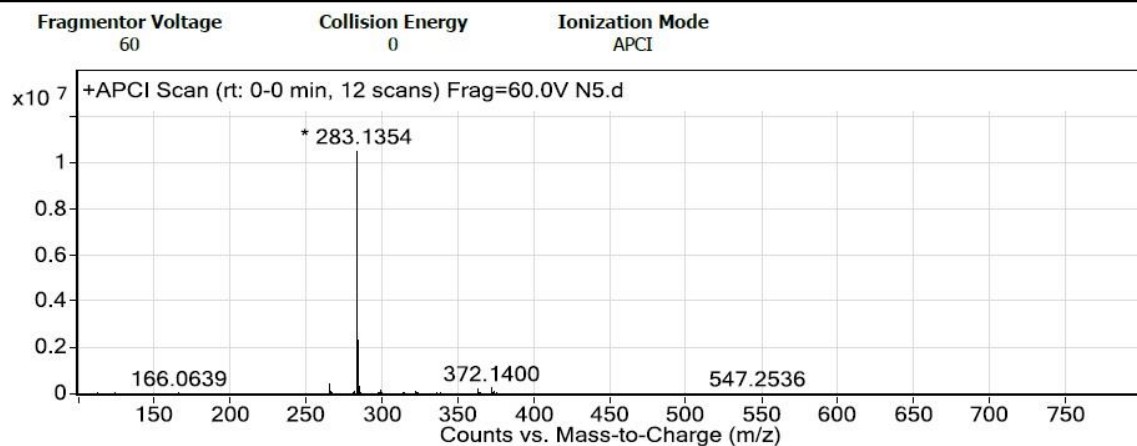


Figure 15. HRMS spectrum of (*E*)-1-(3-hydroxy-4-methoxyphenyl)-5-phenylpent-1-en-3-one (**5e**). (C₁₈H₁₈O₃+H)⁺, Calc: 283.1334.

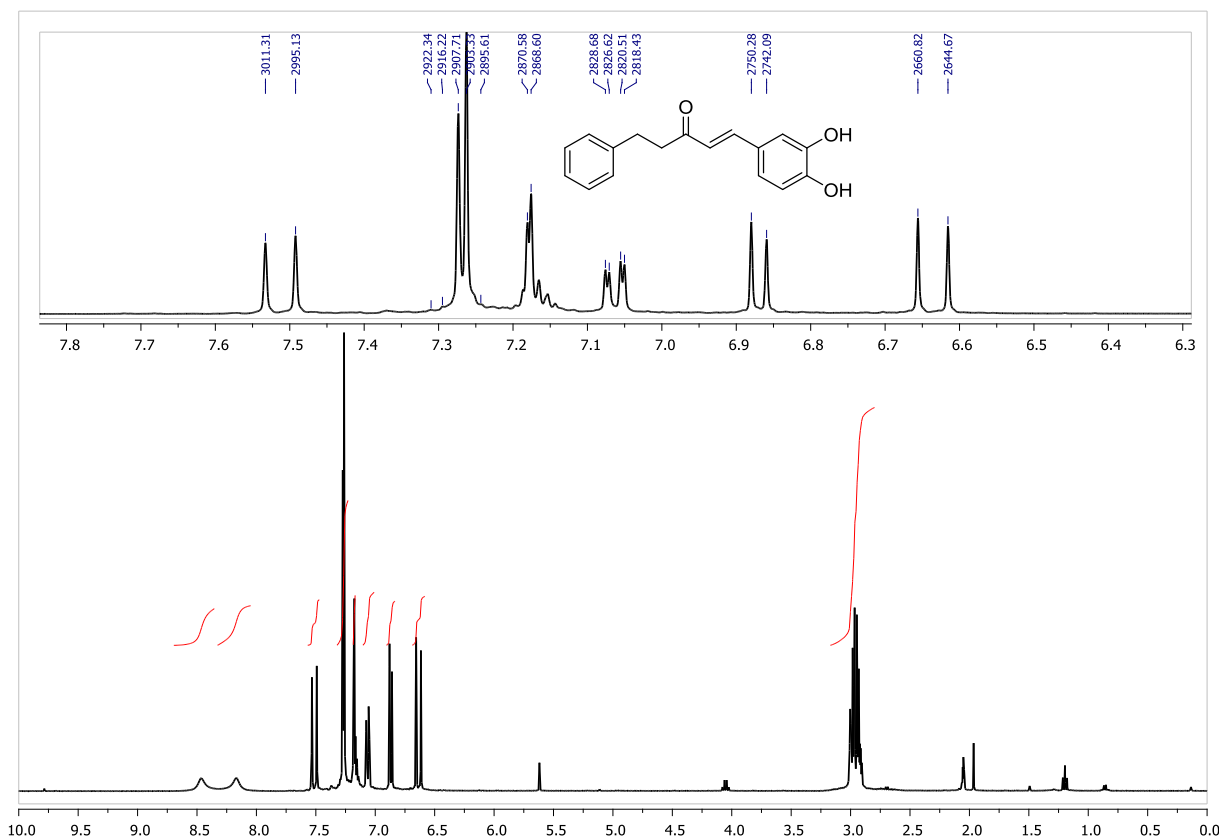


Figure 16. ¹H-NMR spectrum of (*E*)-1-(3,4-dihydroxyphenyl)-5-phenylpent-1-en-3-one (**5f**) (Acetone-d₆).

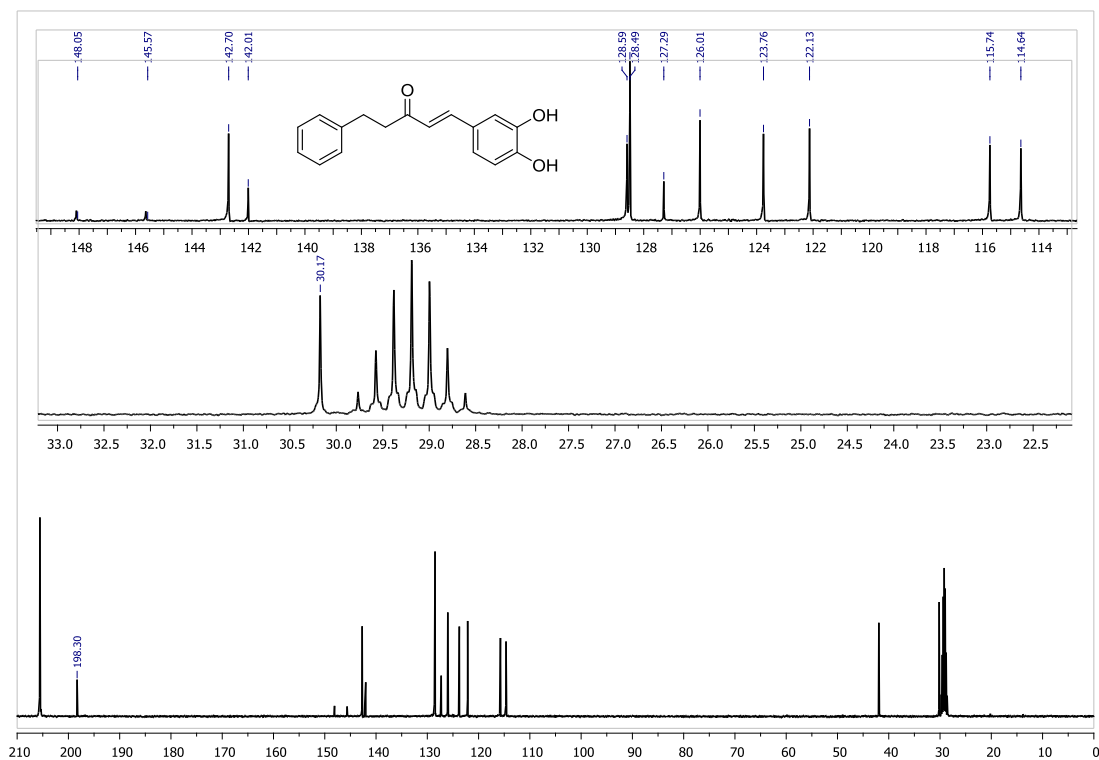


Figure 17. ^{13}C -NMR spectrum of (*E*)-1-(3,4-dihydroxyphenyl)-5-phenylpent-1-en-3-one (**5f**) (Acetone- d_6).

User Spectra

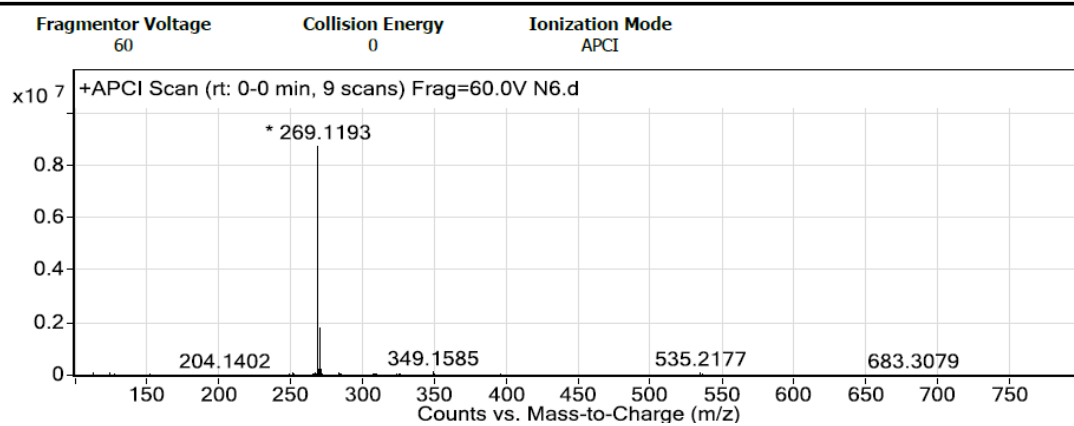


Figure 18. HRMS spectrum of (*E*)-1-(3,4-dihydroxyphenyl)-5-phenylpent-1-en-3-one (**5f**). ($\text{C}_{17}\text{H}_{16}\text{O}_3+\text{H}$) $^+$, Calc: 269.1177.

User Spectra

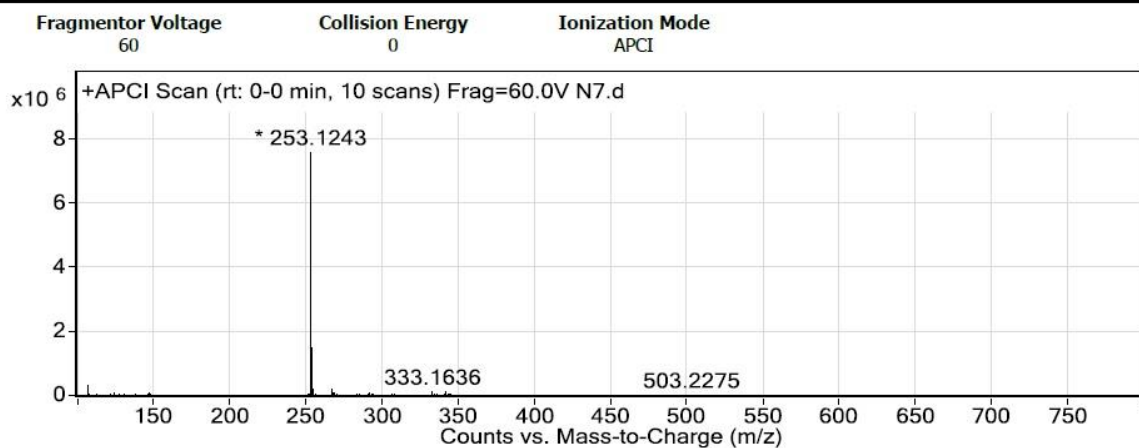


Figure 21. HRMS spectrum of (*E*)-5-(4-hydroxyphenyl)-1-phenylpent-1-en-3-one (**5g**). (C₁₇H₁₆O₂+H)⁺, Calc: 253.1228.

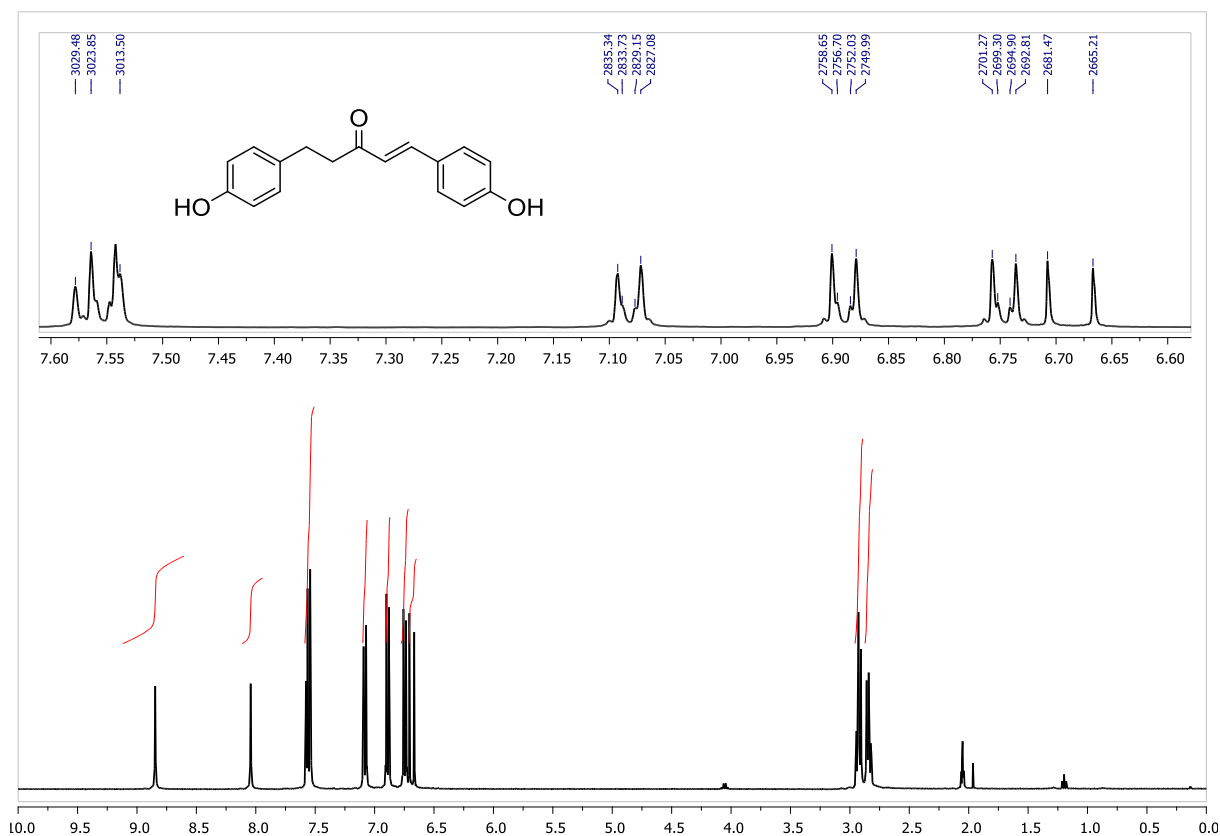


Figure 22. ¹H-NMR spectrum of (*E*)-1,5-bis(4-hydroxyphenyl)pent-1-en-3-one (**5h**) (Acetone-d₆).

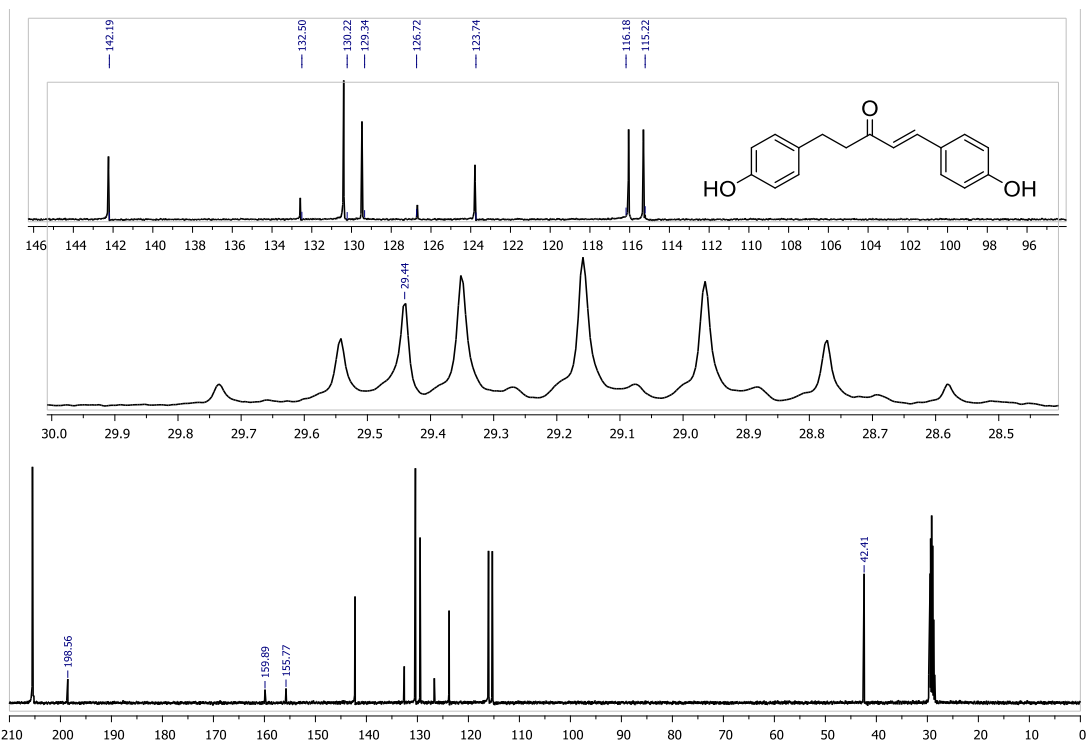


Figure 23. ^{13}C -NMR spectrum of (*E*)-1,5-bis(4-hydroxyphenyl)pent-1-en-3-one (**5h**) (Acetone- d_6).

User Spectra

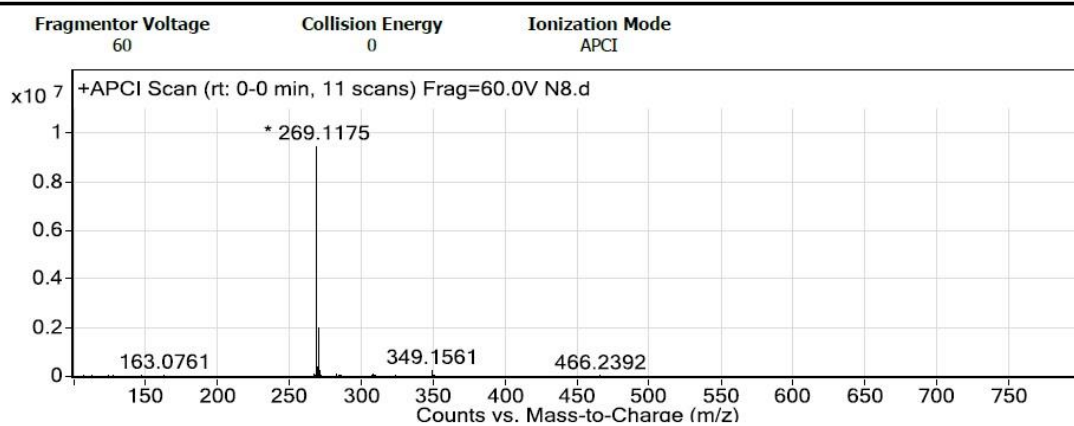


Figure 24. HRMS spectrum of (*E*)-1,5-bis(4-hydroxyphenyl)pent-1-en-3-one (**5h**). $(\text{C}_{17}\text{H}_{16}\text{O}_3+\text{H})^+$, Calc: 269.1177.

User Spectra

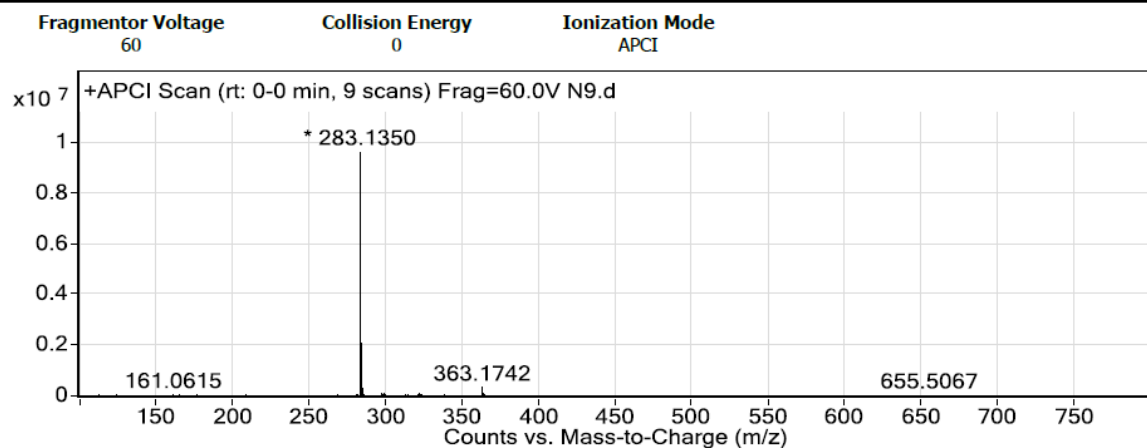


Figure 27. HRMS spectrum of (*E*)-5-(4-hydroxyphenyl)-1-(4-methoxyphenyl)pent-1-en-3-one (**5i**). (C₁₈H₁₈O₃+H)⁺, Calc: 283.1334.

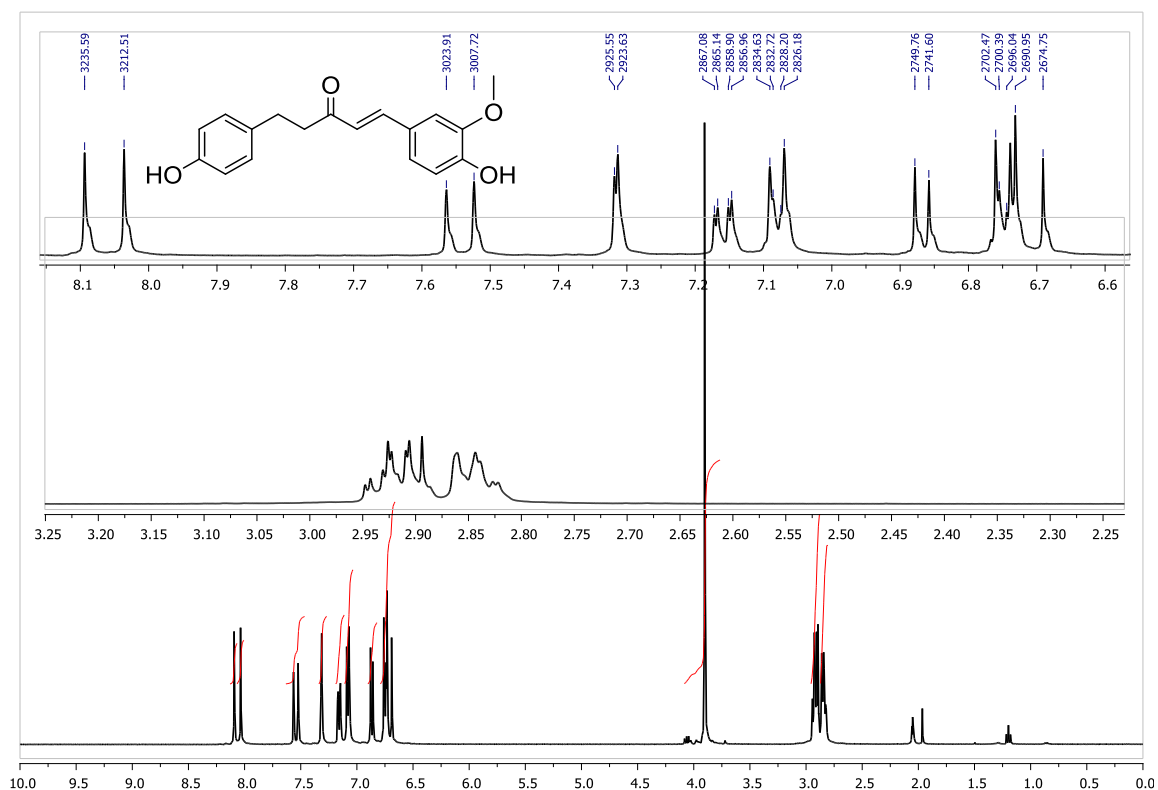


Figure 28. ¹H-NMR spectrum of (*E*)-1-(4-hydroxy-3-methoxyphenyl)-5-(4-hydroxyphenyl)pent-1-en-3-one (**5j**) (Acetone-d₆).

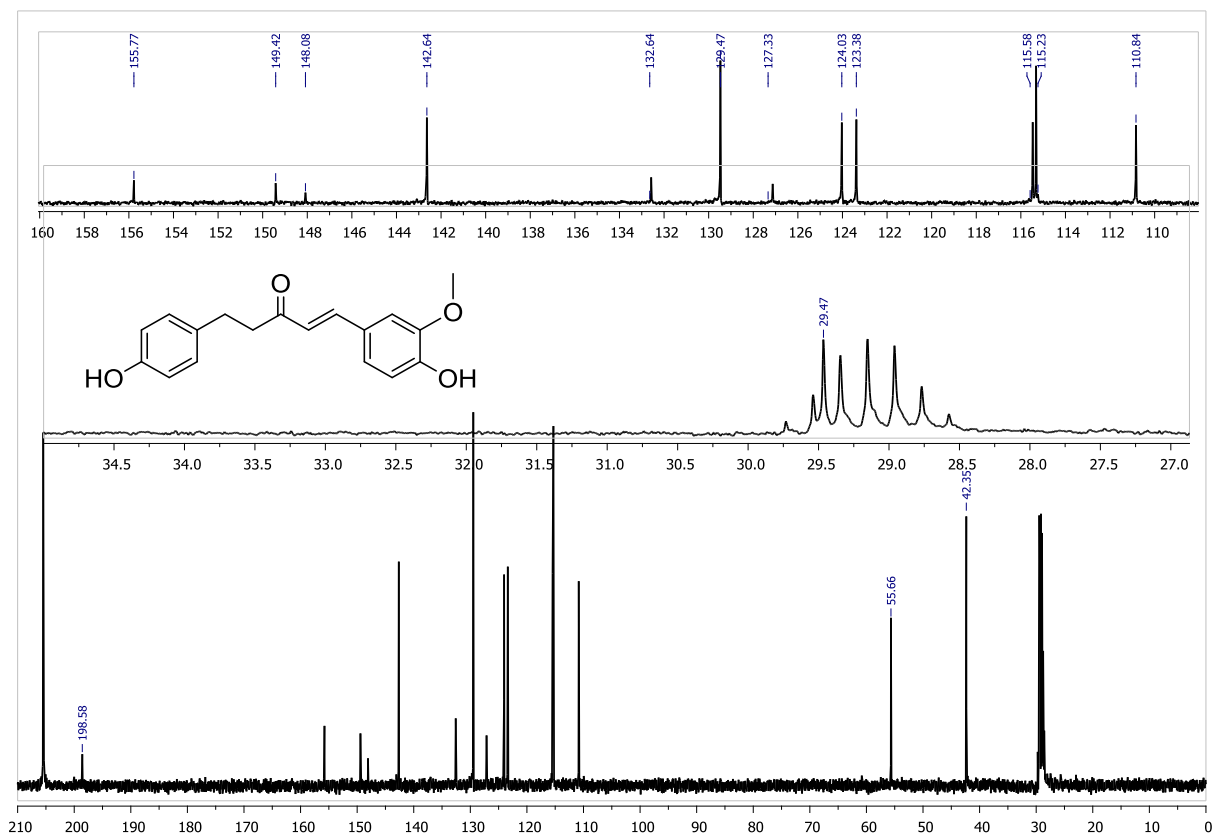


Figure 29. ¹³C-NMR spectrum of (*E*)-1-(4-hydroxy-3-methoxyphenyl)-5-(4-hydroxyphenyl)pent-1-en-3-one (**5j**) (Acetone-*d*₆).

User Spectra

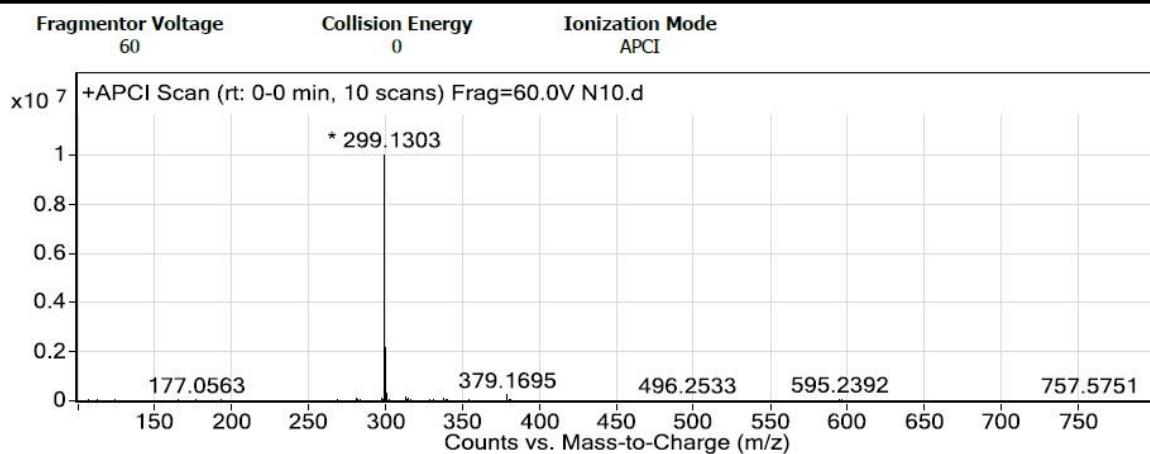


Figure 30. HRMS spectrum of (*E*)-1-(4-hydroxy-3-methoxyphenyl)-5-(4-hydroxyphenyl)pent-1-en-3-one (**5j**). ($C_{18}H_{18}O_4+H$)⁺, Calc: 299.1283.

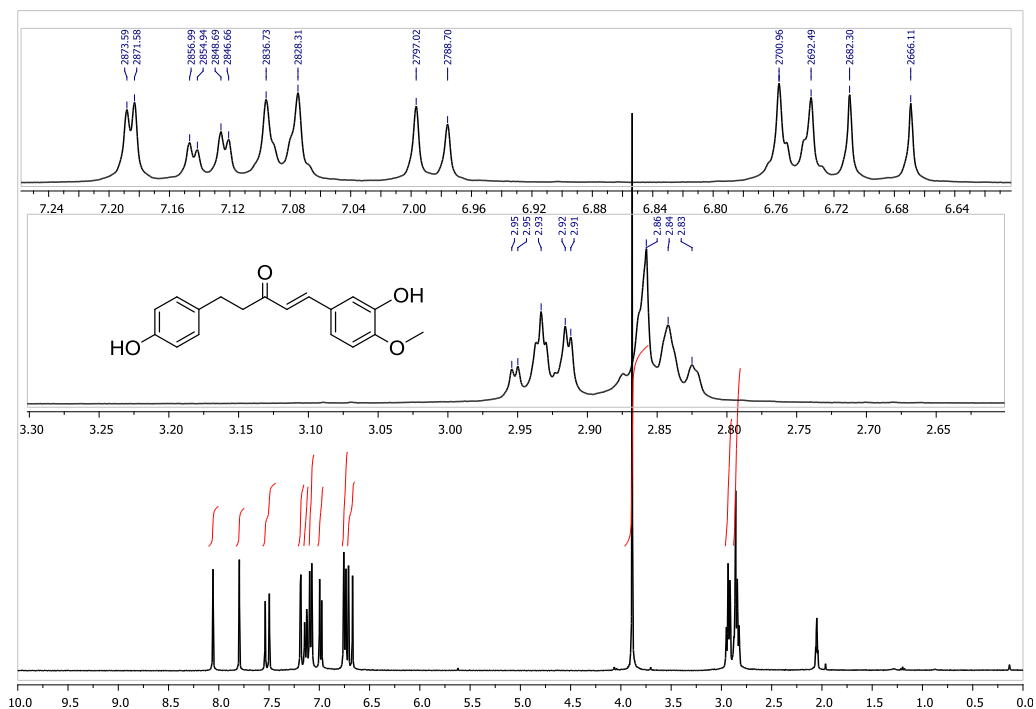


Figure 31. $^1\text{H-NMR}$ spectrum of (*E*)-1-(3-hydroxy-4-methoxyphenyl)-5-(4-hydroxyphenyl)pent-1-en-3-one (**5k**) (Acetone- d_6).

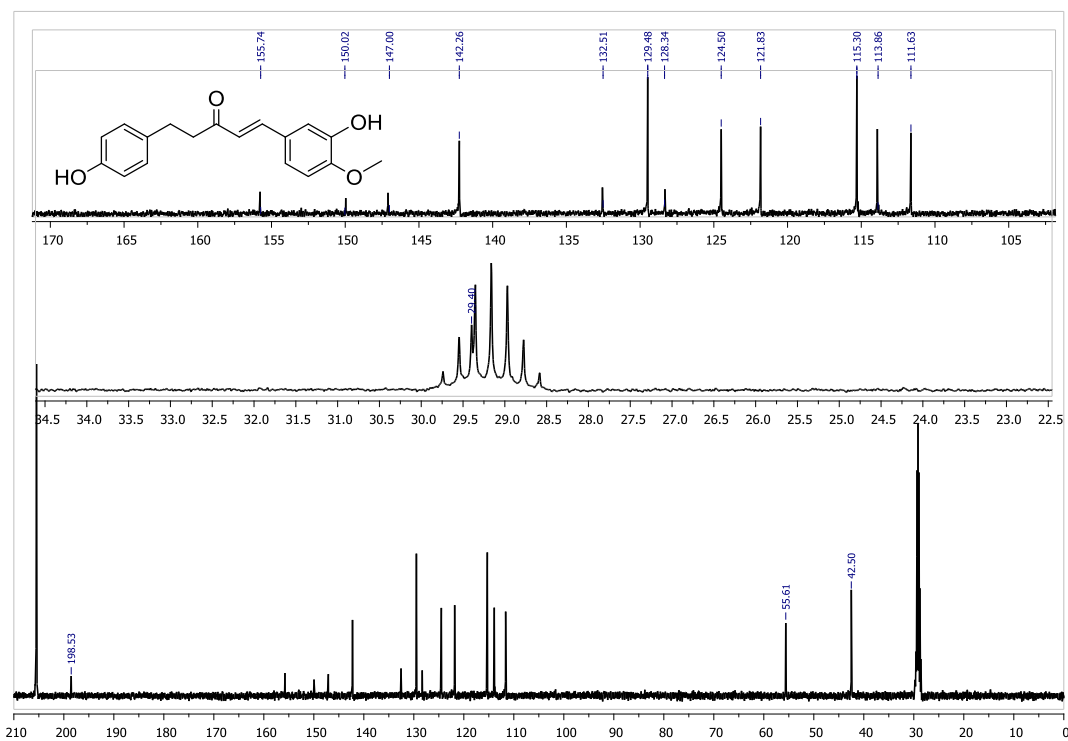


Figure 32. $^{13}\text{C-NMR}$ spectrum of (*E*)-1-(3-hydroxy-4-methoxyphenyl)-5-(4-hydroxyphenyl)pent-1-en-3-one (**5k**) (Acetone- d_6).

User Spectra

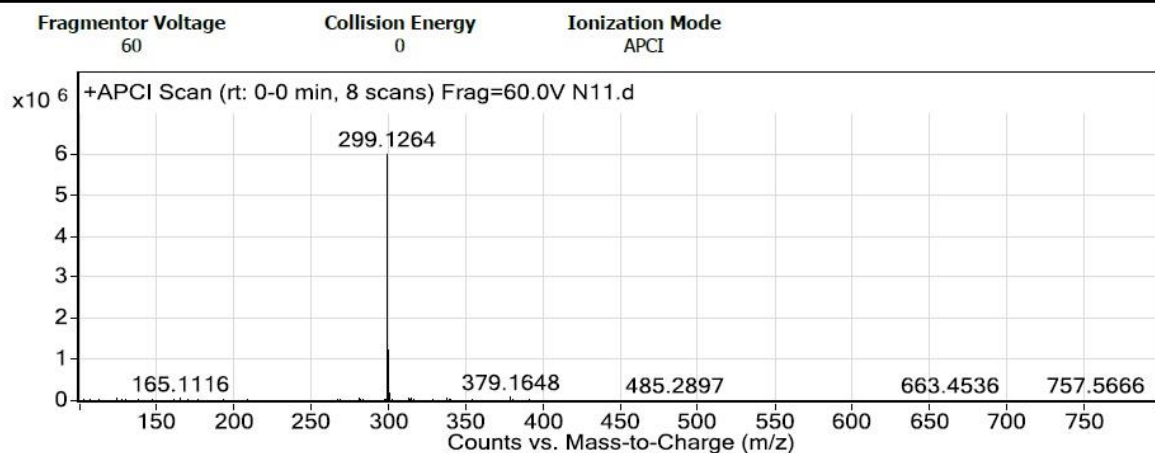


Figure 33. HRMS spectrum of (*E*)-1-(3-hydroxy-4-methoxyphenyl)-5-(4-hydroxyphenyl)pent-1-en-3-one (**5k**). ($C_{18}H_{18}O_4+H$)⁺, Calc: 299.1283.

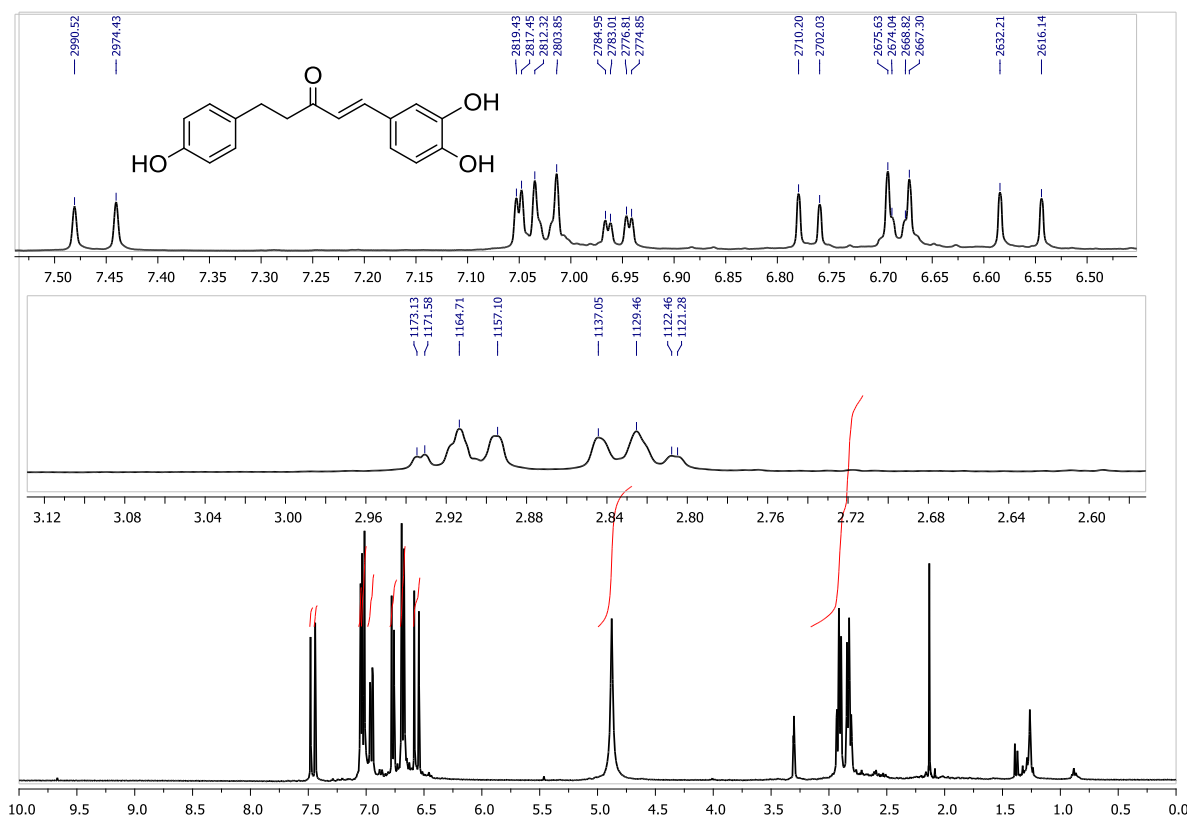


Figure 34. ¹H-NMR spectrum of (*E*)-1-(3,4-dihydroxyphenyl)-5-(4-hydroxyphenyl)pent-1-en-3-one (**5l**) (Methanol-*d*₄).

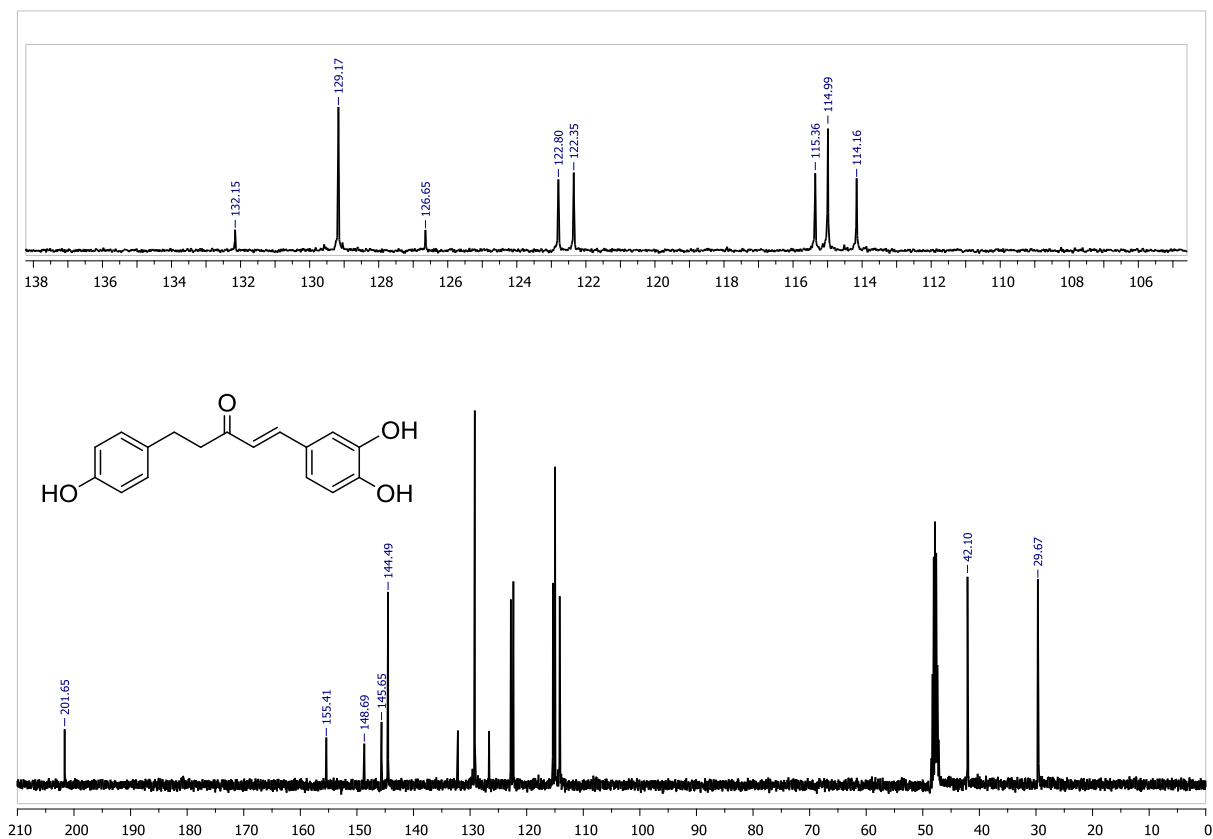


Figure 35. ^{13}C -NMR spectrum of (*E*)-1-(3,4-dihydroxyphenyl)-5-(4-hydroxyphenyl)pent-1-en-3-one (**5I**) (Methanol- d_4).

User Spectra

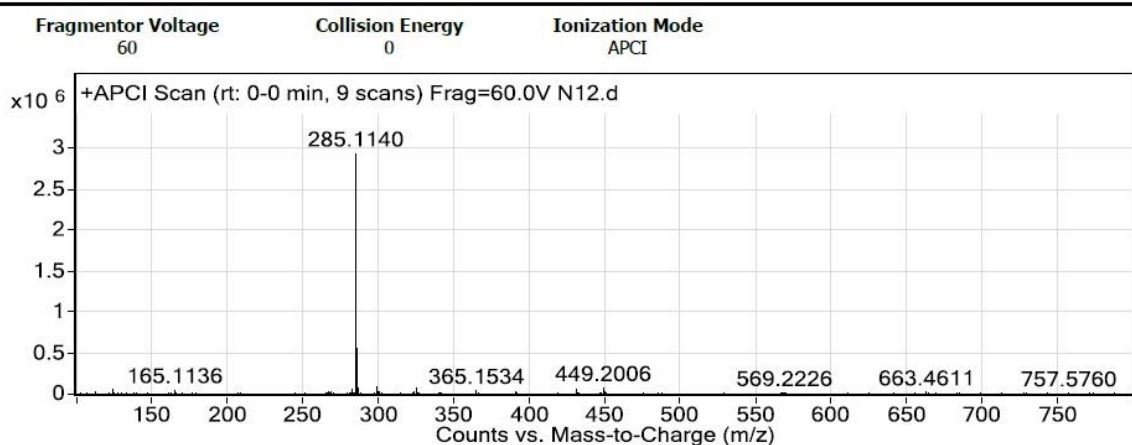


Figure 36. HRMS spectrum of (*E*)-1-(3,4-dihydroxyphenyl)-5-(4-hydroxyphenyl)pent-1-en-3-one (**5I**). $(\text{C}_{17}\text{H}_{16}\text{O}_4+\text{H})^+$, Calc: 285.1126.

Table 1. ¹H-NMR data of compounds 5a–5f (δ (ppm); J (Hz)).

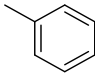
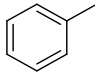
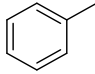
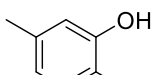
| Compound | Ar ² δ (ppm) | CH ₂ CH ₂ δ (ppm) | H-C(1) δ (ppm) | H-C(2) δ (ppm) | Ar ¹ δ (ppm) |
|----------|---|---|------------------------|------------------------|---|
| 5a |  7.33-7.22 (m, 5H) | 3.02 (A ₂ B ₂ , bs, 4H) | 7.55 (d, 1H, J = 16.2) | 6.74 (d, 1H, J = 16.2) |  7.55-7.52 (m, 2H) 7.41-7.39 (m, 3H) |
| 5b |  7.32-7.18 (m, 5H) | 3.01 (A ₂ B ₂ , bs, 4H) | 7.51 (d, 1H, J = 16.1) | 6.62 (d, 1H, J = 16.1) |  7.43 (d, 2H, J = 8.8) 6.87 (d, 2H, J = 8.8) |
| 5c |  7.32-7.18 (m, 5H) | 3.00 (A ₂ B ₂ , bs, 4H) | 7.51 (d, 1H, J = 16.1) | 6.62 (d, 1H, J = 16.1) |  7.48 (d, 2H, J = 8.4) 6.90 (d, 2H, J = 8.4) 3.84 (s, OMe) |
| 5d |  7.32-7.18 (m, 5H) | 3.00 (A ₂ B ₂ , bs, 4H) | 7.48 (d, 1H, J = 16.3) | 6.59 (d, 1H, J = 16.3) |  7.07 (dd, 1H, J = 8.4, 2.0) 7.03 (d, 1H, J = 2.0) 6.92 (d, 1H, J = 8.4) 5.91 (two s, OH); 3.92 (s, OMe) |
| 5e |  7.32-7.18 (m, 5H) | 3.00-2.96 (A ₂ B ₂ , m 4H) | 7.46 (d, 1H, J = 16.1) | 6.60 (d, 1H, J = 16.1) |  7.14 (d, 1H, J = 2.0) 7.04 (dd, 1H, J = 8.4, 2.0) 6.84 (d, 1H, J = 8.4), 3.92 (s, OMe) 5.72 (s, OH) |
| 5f |  7.32-7.24 (m, 4H) 7.17-7.14 (m, 1H) | 3.00-2.90 (A ₂ B ₂ , m, 4H) | 7.51 (d, 1H, J = 16.1) | 6.64 (d, 1H, J = 16.1) |  8.46 (bs, OH), 8.17 (bs, OH) 7.18 (d, 1H, J = 2.0) 7.07 (dd, 1H, J = 8.2, 2.0) 6.87 (d, 1H, J = 8.2) |

Table 1. Continued

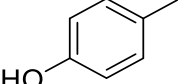
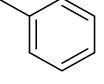
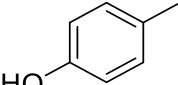
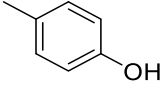
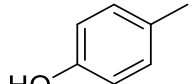
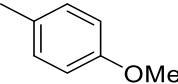
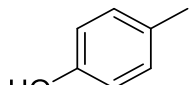
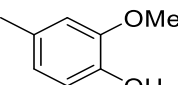
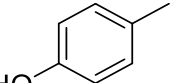
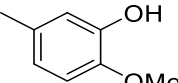
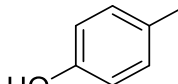
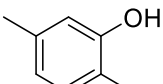
| | | | | | |
|-----------|--|---|---------------------------|---------------------------|--|
| 5g |  HO 7.09 (dm, 2H, $J = 8.4$) 6.77 (dm, 2H, $J = 8.4$) | 3.00-2.94 (A ₂ B ₂ , m, 4H) | 7.54 (d, 1H, $J = 16.4$) | 6.73 (d, 1H, $J = 16.4$) |  7.53-7.51 (m, 2H) 7.41-7.38 (m, 3H) |
| 5h |  HO 8.84 (s, OH), 8.04(s,OH), 7.08 (dm, 2H, $J = 8.4$) 6.74 (dm, 2H, $J = 8.4$) | 2.94-2.90 (A ₂ B ₂ , m, 4H) | 7.56 (d, 1H, $J = 16.1$) | 6.68 (d, 1H, $J = 16.1$) |  7.55 (dm, 2H, $J = 8.4$) 6.88 (dm, 2H, $J = 8.4$) |
| 5i |  HO 8.07 (OH), 7.08 (dm, 2H, $J = 8.8$) 6.74 (dm, 2H, $J = 8.8$) | 2.96-2.82 (A ₂ B ₂ , m, 4H) | 7.58 (d, 1H, $J = 16.2$) | 6.72 (d, 1H, $J = 16.2$) |  7.63 (dm, 2H, $J = 8.8$) 6.98 (dm, 2H, $J = 8.8$), 3.84 (s, OMe) |
| 5j |  HO 8.09 (OH), 7.08 (dm, 2H, $J = 8.4$) 6.75 (dm, 2H, $J = 8.4$) | A ₂ part 2.94-2.82 (A ₂ B ₂ , m, 4H) | 7.54 (d, 1H, $J = 16.2$) | 6.71 (d, 1H, $J = 16.2$) |  8.03 (OH) 7.31 (d, 1H, $J = 1.9$) 7.16 (dd, 1H, $J = 8.2, 1.9$) 6.87 (d, 1H, $J = 8.2$), 3.90 (s, OMe) |
| 5k |  HO 8.05(OH), 7.09 (dm, 2H, $J = 8.4$) 6.75 (dm, 2H, $J = 8.4$) | 2.95-2.82 (A ₂ B ₂ , m, 4H) | 7.51 (d, 1H, $J = 16.2$) | 6.69 (d, 1H, $J = 16.2$) |  7.79 (OH), 7.19(d, 1H, $J = 2.0$) 7.13 (dd, 1H, $J = 8.3, 2.0$) 6.99 (d, 1H, $J = 8.3$), 3.88 (s, OMe) |
| 5l |  HO 7.02 (dm, 2H, $J = 8.4$) 6.68 (dm, 2H, $J = 8.4$) | 2.94--2.80 (A ₂ B ₂ , m, 4H) | 7.46 (d, 1H, $J = 16.1$) | 6.56 (d, 1H, $J = 16.1$) |  7.05 (d, 1H, $J = 1.9$) 6.95 (dd, 1H, $J = 8.2, 1.9$) 6.77 (d, 1H, $J = 8.2$), 4.87 (bs, 2 x OH) |

Table 2. ¹³C-NMR data of 5a–5f (δ (ppm); J (Hz)).^{a,b} Exchangeable carbons.

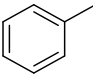
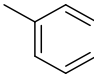
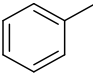
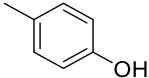
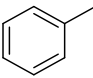
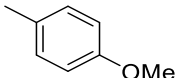
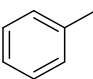
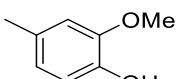
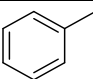
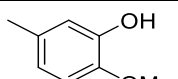
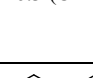
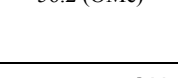
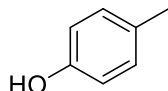
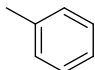
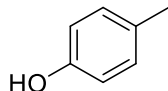
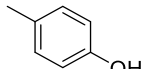
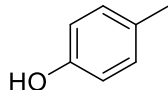
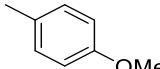
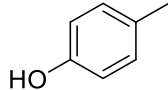
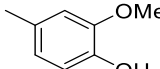
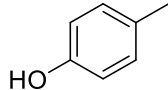
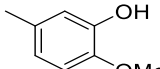
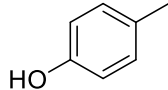
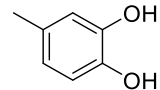
| Compound | Ar ² | C(5) | C-(4) | C-(3) | C-(2) | C-(1) | Ar ¹ |
|----------|---|------|-------|-------|-------|-------|--|
| 5a |  141.5 (C-1'') 128.6 ^a (C-2''/6'') 128.5 ^a (C-3''/5'') 126.4 (C-4'') | 30.4 | 42.7 | 199.6 | 126.4 | 142.9 |  134.7 (C-1') 129.2 ^a (C-2'/6') 128.8 ^a (C-3'/5') 130.7 (C-4') |
| 5b |  141.4 (C-1'') 128.8 ^a (C-2''/6'') 128.6 ^a (C-3''/5'') 126.4 (C-4'') | 30.6 | 42.5 | 200.5 | 123.9 | 143.5 |  127.1 (C-1') 130.6 (C-2'/6') 116.3 (C-3'/5') 158.6 (C-4') |
| 5c |  141.6 (C-1'') 128.7 ^a (C-2''/6'') 128.6 ^a (C-3''/5'') 126.3 (C-4'') | 30.5 | 42.6 | 199.5 | 124.2 | 142.7 |  127.3 (C-1') 130.2 (C-2'/6') 114.6 (C-3'/5') 161.8 (C-4'), 55.6 (OMe) |
| 5d |  141.5 (C-1'') 128.7 ^a (C-2''/6'') 128.6 ^a (C-3''/5'') 126.3 (C-4'') | 30.5 | 42.4 | 199.5 | 123.7 | 143.2 |  127.2 (C-1'), 109.6 (C-2') 148.4 (C-3'), 147.0 (C-4') 115.0 (C-5'), 124.2 (C-6'), 56.2 (OMe) |
| 5e |  141.5 (C-1'') 128.7 ^a (C-2''/6'') 128.6 ^a (C-3''/5'') 126.3 (C-4'') | 30.5 | 42.7 | 199.5 | 122.4 | 142.9 |  128.3 (C-1'), 110.8 (C-2') 149.0 (C-3'), 146.1 (C-4') 113.3 (C-5'), 124.7 (C-6'), 56.2 (OMe) |
| 5f |  142.0 (C-1'') 128.6 ^a (C-2''/6'') 128.5 ^a (C-3''/5'') 126.0 (C-4'') | 30.2 | 41.9 | 198.3 | 123.8 | 142.7 |  127.3 (C-1'), 114.6 (C-2') 148.0 (C-3'), 145.6 (C-4') 115.7 (C-5'), 122.1 (C-6') |

Table 2. Continued

| | | | | | | | |
|-----------|---|------|------|-------|-------|-------|---|
| 5g |  HO 133.3 (C-1'') 129.7 (C-2''/6'') 115.5 (C-3''/5'') 154.3 (C-4'') | 29.6 | 42.9 | 200.3 | 126.2 | 143.2 |  134.7 (C-1') 129.2 ^a (C-2'/6') 128.5 ^a (C-3'/5') 130.7 (C-4') |
| 5h |  HO 132.5 (C-1'') 129.3 ^a (C-2''/6'') 115.2 ^b (C-3''/5'') 155.8 (C-4'') | 29.4 | 42.4 | 198.6 | 123.7 | 142.2 |  126.7 (C-1') 130.2 ^a (C-2'/6') 116.2 ^b (C-3'/5') 159.9 (C-4') |
| 5i |  HO 132.4 (C-1'') 129.3 ^a (C-2''/6'') 114.6 ^b (C-3''/5'') 155.7 (C-4'') | 29.4 | 42.4 | 198.6 | 124.5 | 141.8 |  127.6 (C-1') 130.2 ^a (C-2'/6') 115.5 ^b (C-3'/5') 161.9 (C-4') 55.1 (OMe) |
| 5j |  HO 132.6 (C-1'') 129.5 (C-2''/6'') 115.2 (C-3''/5'') 155.8 (C-4'') | 29.5 | 42.4 | 198.6 | 124.0 | 142.6 |  127.3 (C-1'), 110.8 (C-2') 149.4 (C-3'), 148.1 (C-4') 115.6 (C-5'), 123.4 (C-6'); 55.7 (OMe) |
| 5k |  HO 132.5 (C-1'') 129.5 (C-2''/6'') 113.9 (C-3''/5'') 155.7 (C-4'') | 29.4 | 42.5 | 198.5 | 124.5 | 142.3 |  128.3 (C-1'), 111.6 (C-2') 150.0 (C-3'), 147.0 (C-4') 115.3 (C-5'), 121.8 (C-6'), 55.6 (OMe). |
| 5l |  HO 132.2 (C-1'') 129.2 (C-2''/6'') 115.0 (C-3''/5'') 155.4 (C-4'') | 29.7 | 42.1 | 201.7 | 122.8 | 144.5 |  126.6 (C-1'), 114.2 (C-2') 148.7 (C-3'), 145.7 (C-4') 115.4 (C-5'), 122.4 (C-6') |